DEL-SG-28-89

A Numerical Scheme Using A Transmutation Approach for Underwater Sound Propagation

$2.00

by

Robert P. Gilbert
Dept. of Math. Sciences
University of Delaware
Newark, DE 19716, USA

Yongzhi Xu
Dept. of Math. Sciences
University of Delaware
Newark, DE 19716, USA

David Wood
Dept. of Comp. & Info. Services
University of Delaware
Newark, DE 19716

October 1989

University of Delaware Sea Grant College Program
Newark, DE 19716

This publication is the result of research sponsored by NOAA Office of Sea Grant, Department of Commerce, under Grant No. NA86AA-D-SG040 (Project No. R/OE-2). The U.S. Government is authorized to produce and distribute reprints for governmental purposes, notwithstanding any copyright notation that may appear hereon.

The University of Delaware Sea Grant College Program is supported cooperatively by the National Oceanic and Atmospheric Administration, U.S. Department of Commerce, and by the State of Delaware.

A Numerical Scheme Using a Transmutation Approach for Underwater Sound Propagation

Robert P. Gilbert, Yongzhi Xu
Dept. of Math. Sciences ,
David Wood
Dept. of Comp. & Information Sciences,
University of Delaware ,
Newark , DE 19716 . [1]

1. Introduction

In [8] we have described a procedure for solving the ***submersible identification problem*** in three steps. That is, for the first approximation we shall concentrate on an ocean which may be taken to be a slab of thickness h, R^3_h, and has a constant index of refraction. This is reasonable as the most difficult aspects of our problem come from the way the ocean surface interferes with the propagation of sound off an arbitrary submersible.[6], [8] Because of the difficulties introduced by the ocean boundaries, analytical computation of the far field must be based on some sort of approximation scheme such as using a parabolic approximation, which tends to destroy vertical resolution; or using a trucated form of the modal expansion for the Green's function (propagator):

$$G(r,\theta,z;\rho,\phi,\zeta) = \frac{i\pi}{2}\sum_{n=0}^{\infty}\frac{\phi_n(z)\phi_n(\zeta)}{\|\phi_n\|^2}H_0(ka_n \mid re^{i\theta} - \rho e^{i\phi} \mid). \qquad (1.1)$$

Here the $a_n = [1-(n+1/2)^2(\pi/kh)^2]^{-1/2}$ are the modal eigenvalues and $\phi_n(z) = sin(k(1-a_n^2)^{1/2}z)$[1]. By using the propagator $G(r,z;\rho,\zeta)$ (1.1),

[1] This work is supported in part by Sea Grant NA86AA-D-SG040.

the Green's integral representation, and the asymptotic behavior of the Hankel functions, Gilbert and Xu[5], [6] have shown that the acoustic pressure has the asymptotic expansion

$$p(r,z,\theta) = \frac{1}{r^{1/2}} \sum_{n=0}^{\infty} e^{ika_n r} \sum_{m=0}^{\infty} \frac{f_{nm}(z,\theta)}{r^m}$$

$$\simeq \frac{1}{r^{1/2}} \sum_{m=0}^{\infty} \frac{F_m(r,z,\theta)}{r^m}, \tag{1.2}$$

where

$$F_m(r,z,\theta) := \sum_{n=0}^{N} e^{ika_n r} F_{nm}(z,\theta). \tag{1.3}$$

The modes $\phi_n(z)$ for $n > N$ do not propagate, but rather decay exponentially and hence are not included in the sum (1.3). We refer to the term

$$F_0(r,z,\theta) := \sum_{n=0}^{N} e^{ika_n r} F_{n0}(z,\theta) \tag{1.4}$$

as the finite-ocean far field pattern, which we also write in an array form as

$$F(z,\theta) := [f_{00}(z,\theta),\ f_{10}(z,\theta), ..., f_{N0}(z,\theta)].$$

Gilbert and Xu [5],[6] show that it has a modal representation of form

$$\nu(\mathbf{x},z) := \sum_{n=0}^{N} \frac{\phi_n(\zeta)}{\|\phi_n\|^2 \sqrt{a_n}} \int_{\partial Z_1} g(z,\phi)\phi_n(z) e^{ika_n \langle \mathbf{x},\xi \rangle} d\sigma_\xi, \tag{1.5}$$

where $g(z,\phi)$ is called a propagating Herglotz kernel.

Having obtained an approximate far field pattern for various wave numbers k and various z dependencies in the incident "plane waves", in step two we may solve the inverse problem. Recall that the "plane waves" have modal components in the z direction. If we are not considering axially symmetric solutions then for each modal component and for each k we use 2n+1 incoming waves with directions in the range coordinates

$$\alpha_2^j = [cos(2\pi j/(2n+1)), sin(2\pi j/(2n+1))]\,,\; j = 0, 1, 2, ..., 2n \qquad (1.6)$$

Now let F^j_{nm} $0 \le n \le N,\ -n \le m \le n$ be the coefficients of the spherical harmonic approximation of far field pattern F^j generated by the plane wave with the direction α_j. By expanding the propagating Herglotz kernels, and the parametric representation of the submersible's surface $\rho = f(\theta, \phi)$ in terms of surface harmonics we are led to consider a minimization problem of the form

$$\mu(F) = \min_{(k^2, g, \rho)} \{ \sum_{j=1}^{2n} \left| \int_{\partial Z_1} F(z, \phi; k, \alpha_2^{(j)}) g(z, \phi) dz d\phi \right|^2$$

$$+ \int_0^{2\pi} \int_0^{\pi} \left| T^{-1} V(f(\phi, \theta), \phi, \theta) \right|^2 sin^2\theta d\theta d\phi \}, \qquad (1.7)$$

where

$$V(y) := \sqrt{\frac{2}{ik\pi}} \int_{\partial Z_1} g(z, \phi) G(\mathbf{x}, z, \xi, \zeta) d\sigma_\xi$$

is the propagating (entire) Herglotz function, and T^{-1} is the inverse transformation which relates the coefficients of the starting field in spherical coordinates to those in cylindrical coordinates. Other minimization problems might be considered instead, for example see Xu [10].

In step three, we consider the case with an index of refraction which is depth dependent. We must make certain alternations in STEP ONE and STEP TWO. In this step we need to find a complete system of the solutions to replace the complete family (1.9) by another one, which must be a solution of the depth-dependent Helmholtz equation

$$\Delta u + k^2 n^2(z) u = 0. \qquad (1.8)$$

Such a family may be generated by means of the transmutation

$$\Xi\Omega := \Omega(r,z,\phi) + \int_{z=h}^{z} K(z,s)\Omega(r,s,\phi)ds,$$

where the kernel K(z,s) satisfies the Gelfand-Levitan equation

$$\frac{\partial^2 K}{\partial z^2} - \frac{\partial^2 K}{\partial s^2} + k^2[n^2(z) - 1]K = 0, \tag{1.9}$$

and the characteristic conditions [4]

$$2\frac{\partial}{\partial z}K(z,z) + k^2[n^2(z) - 1] = 0, \tag{1.10}$$

$$2\frac{\partial}{\partial z}K(z,-z+2h) + k^2[n^2(z) - 1] = 0, \tag{1.11}$$

that characterize a hard ocean boundary at z=h. The functions $\Omega(r,z)$ are solutions of (1.8) with n(z)=1 and boundary conditions. In order to obtain the propagating far-field patterns, we represent the propagating solution by

$$\sum_{n=0}^{N_2} \sum_{m=-M}^{M} \beta_{mn}\phi_n(z)H_m^{(1)}(ka_n r)e^{im\theta}, \tag{1.12}$$

where the $\phi_n(z)$ are the modal solutions (eigenfunctions of the separated z-equation) for the variable index $n(z)$:[4], [6]

$$q_{zz} + k^2(n^2(z) - a^2)q = 0, \tag{1.13}$$

and the boundary conditions

$$q_z(ka,h) = 0, \tag{1.14}$$

and

$$q(ka,0) = 0. \tag{1.15}$$

It is clear that if we want to study the wave propagation and its far-field patterns, we must know the normal modes in the stratified ocean. Therefore, as an important component of step three, we need to construct $\phi_n(z)$, $n = 0, 1, 2, \ldots$ numerically for $n(z) \neq 1$.

2 Numerical Transmutation Method

As discussed in [4], a solution of (1.13)$\sim$ (1.15) is given by

$$q_1(ka, z) = p_1(ka, z) + \int_h^z K(z, s)p_1(ka, s)ds \tag{2.1}$$

where $K(z, s)$ is a solution of (1.9) $\sim$ (1.11) and $p(ka, z)$ satisfies

$$p_{zz} + k^2(1 - a^2)p = 0, \tag{2.2}$$

and the boundary condition

$$p_z(ka, h) = 0. \tag{2.3}$$

Notice that $q_1(ka, z)$ will satisfy the boundary condition (1.14) at z=h regardless of the value of a because $p_1(ka, z)$ has the same property and our transmutation preserves boundary conditions at z=h. The boundary condition (1.15) at z=0 is then used to determine the values of a_n that are roots of

$$p_1(ka, 0) + \int_h^0 K(0, s)p_1(ka, s)ds = 0. \tag{2.4}$$

Since $n(z)$ may be ≥ 1 or ≤ 1 in general, we may have that $a_n^2 \geq 1$ or $a_n^2 \leq 1$. In fact, there is a documented example [13] where

$$n^2(z) = 1 - 0.1cos(\frac{2\pi z}{h}),$$

where $h = 2000, k = 8\pi/2000$, for which we have

$$(ka_0)^2 = 1.6555156 \times 10^{-4},$$

$$(ka_1)^2 = 1.5101910 \times 10^{-4},$$

that is,

$$a_0^2 = 1.0483675 > 1,$$

$$a_1^2 = 0.9563396 < 1.$$

Therefore, $p_1(ka, z)$ may generally be given by either

$$p_1(ka, z) := cos[k(1 - a^2)^{1/2}(h - z)], if\ a < 1, \tag{2.5}$$

or

$$p_1(ka, z) := cosh[k(a^2 - 1)^{1/2}(h - z)],\ if\ a > 1. \tag{2.6}$$

For $a^2 < 1$, let $\lambda = k(1 - a^2)^{1/2}h$, (2.4) becomes

$$cos(\lambda) + \int_h^0 K(0, s)cos[\lambda(1 - \frac{s}{h})]ds = 0. \tag{2.7}$$

For $a^2 > 1$, let $\lambda = k(a^2 - 1)^{1/2}h$, (2.4) becomes

$$cosh(\lambda) + \int_h^0 K(0, s)cosh[\lambda(1 - \frac{s}{h})]ds = 0. \tag{2.8}$$

Obviously, in order to find all propagating eigenvalues we have to find all $\lambda \geq 0$ such that either (2.7) or (2.8) is satisfied. To avoid this inconvenience, we can rewrite the equation (1.13) as

$$q_{zz} + k^2[(n^2(z) - n_0^2) - (a^2 - n_0^2)]q = 0, \tag{2.9}$$

where $n_0^2 > 0$ can be chosen so that $a^2 < 1 + n_0^2$.

Let $\hat{n}^2(z) = n^2 - n_0^2,\ \hat{a}^2 = a^2 - n_0^2$, the solution of (2.9) can be written as

$$q(k\hat{a}, z) = p(k\hat{a}, z) + \int_h^z \hat{K}(z, s)p(k\hat{a}, s)ds \tag{2.10}$$

where $\hat{K}(z, s)$ satisfies

$$\frac{\partial^2 \hat{K}}{\partial z^2} - \frac{\partial^2 \hat{K}}{\partial s^2} + k^2[n^2(z) - n_0^2 - 1]\hat{K} = 0, \tag{2.11}$$

and the characteristic conditions [4]

$$2\frac{\partial}{\partial z}\hat{K}(z, z) + k^2[n^2(z) - n_0^2 - 1] = 0, \tag{2.12}$$

$$2\frac{\partial}{\partial z}\hat{K}(z, -z + 2h) + k^2[n^2(z) - n_0^2 - 1] = 0. \tag{2.13}$$

The eigenvalues are the roots of equation (2.7) with $\lambda = k(1 - \hat{a}^2)^{1/2}h$. We can normalize the problem by letting $\hat{z} = z/h,\ \hat{s} = s/h,\ \xi = (\hat{z} + \hat{s} - 2)/2,\ and\ \eta = (\hat{z} - \hat{s})/2,\ k = k_0 h$; then (2.11) $\sim$ (2.13) can be reduced to

$$\frac{\partial^2 M}{\partial\xi\partial\eta} + k^2[n^2(1 - \xi - \eta) - n_0^2 - 1]M = 0,\ \ 0 \le \xi + \eta \le 1, \tag{2.14}$$

$$M(\xi, 0) = \frac{1}{2}k^2 \int_0^\xi [n^2(1 - t) - n_0^2 - 1]dt,\ 0 \le \xi \le 1, \tag{2.15}$$

$$M(0, \eta) = \frac{1}{2}k^2 \int_0^\eta [n^2(1 - t) - n_0^2 - 1]dt,\ 0 \le \eta \le 1. \tag{2.16}$$

We use a finite difference method developed in [2] to compute $M(\xi, \eta)$ as well as $K(z, s)$. Following Aziz and Hubbard [2], we define for $0 \le m + n \le L$, where L is the number of interpolation points and $dz = 1/L$, we see that

$$M(mdz - \frac{1}{2}dz, ndz) = \frac{1}{2}[M(mdz, ndz) + M(mdz - dz, ndz)],$$

$$M(mdz, ndz - \frac{1}{2}dz) = \frac{1}{2}[M(mdz, ndz) + M(mdz, ndz - dz)],$$

$$M(mdz-\frac{1}{2}dz,ndz-\frac{1}{2}dz)=$$
$$\frac{1}{2}[M(mdz-\frac{1}{2}dz,ndz)+M(mdz-\frac{1}{2}dz,ndz-dz)]$$
$$=\frac{1}{2}[M(mdz,ndz-\frac{1}{2}dz)+M(mdz-dz,ndz-\frac{1}{2}dz)]$$
$$=\frac{1}{4}[M(mdz,ndz)+M(mdz-dz,ndz)$$
$$+M(mdz,ndz-dz)+M(mdz-dz,ndz-dz)],$$
$$M_{\xi\eta}(mdz-\frac{1}{2}dz,ndz-\frac{1}{2}dz)$$
$$=(dz)^{-2}[M(mdz,ndz)-M(mdz-dz,ndz)$$
$$-M(mdz,ndz-dz)+M(mdz-dz,ndz-dz)],$$

where

$$c_{mn}=k^2[n^2(Ndz-(m+n-1)dz)-n_0^2-1],$$

Now (2.14) may be approximated by

$$(dz)^{-2}[M(mdz,ndz)-M(mdz-dz,ndz)-M(mdz,ndz-dz)$$
$$+M(mdz-dz,ndz-dz)]+c_{mn}\frac{1}{4}[M(mdz,ndz)+M(mdz-dz,ndz)$$
$$+M(mdz,ndz-dz)+M(mdz-dz,ndz-dz)]=0.$$

Denote $u_{mn}=M(mdz,ndz)$, then

$$u_{mn}=\frac{4-c_{mn}(dz)^2}{4+c_{mn}(dz)^2}u_{m(n-1)}+\frac{4-c_{mn}(dz)^2}{4+c_{mn}(dz)^2}u_{(m-1)n}-u_{(m-1)(n-1)}, \quad (2.17)$$

with

$$u_{m0}=f(mdz-\frac{1}{2}dz), \quad (2.18)$$

and

$$u_{0n}=g(ndz-\frac{1}{2}dz), \quad (2.19)$$

where

$$f(\xi) = \frac{k^2}{2}\int_0^\xi [n^2(1-t) - n_0^2 - 1]dt,\ 0 \le \xi \le 1,$$
$$g(\eta) = \frac{k^2}{2}\int_0^\eta [n^2(1-t) - n_0^2 - 1]dt,\ 0 \le \eta \le 1.$$

As showed in [2], the global error of this scheme is $O((1/L)^2)$. A FORTRAN program using this scheme is in Appendix A.

We can also use finite difference approximation to the equation (2.1) as well as (2.12)(2.13). Let $dz = ds = 1/l$,

$$K_{zz}(idz, ids) = \frac{1}{dz^2}(K_{i+1,j} - 2K_{i,j} + K_{i-1,j}),$$
$$K_{ss}(idz, ids) = \frac{1}{dz^2}(K_{i,j+1} - 2K_{i,j} + K_{i,j+1}),$$
$$K(idz, ids) = \frac{1}{2}(K_{i,j+1} + K_{i,j-1}),$$

then (2.11) follows

$$K_{i+1,j} + K_{i-1,j} - K_{i,j+1} - K_{i,j-1} + (dz)^2[n^2(i) - n0 - 1](K_{i,j+1} + K_{i,j-1}) = 0, \tag{2.20}$$

$$0 \le i + j \le 2L,\ \ j \ge i \ge 0$$

and

$$K_{i,i} = -\frac{k^2(dz)}{2}\left[\frac{\hat{n}^2(i) + \hat{n}^2(0) - 2}{2} + \sum_{j=1}^{i-1}(\hat{n}^2(j) - 1)\right],$$
$$K_{i,2L-i} = -\frac{k^2(dz)}{2}\left[\frac{\hat{n}^2(i) + \hat{n}^2(0) - 2}{2} + \sum_{j=1}^{i-1}(\hat{n}^2(j) - 1)\right],$$
$$fori = 1, 2, ..., 2L.$$

A PC-Matlab program using this scheme is shown in Appendix B.

3 Examples

In this section we present two examples and compare them with typical normal mode computation results.

Example 1: The results presented in this example are based on an idealized ocean model with a symmetric sound channel. The index of refraction is

$$n^2(z) = 1 - 0.1cos(\frac{2\pi z}{h}),$$

where the depth of ocean $h = 2000$, and $k = 8\pi/2000$.

Figure 1: The transmutation kernel $K(z, s)$ for example 1.

Figure 2: The eigenvalues shown bracketed by two os, which are the zeros of

$$cos(\lambda) + \int_h^0 K(0, s)cos[\lambda(1 - \frac{s}{h})]ds = 0.$$

The dotted curve is $cos(\lambda)$ and the solid curve is the integral term.

Table 1: Unperturbed eigenvalues ($\times 10^{-3}$) for example 1. The index of refraction $n^2(z) = 1$.

TABLE 1: (x10e-3)

Mode	DSF analytic	TRSM fortran	TRSMf error	TRSM MC-Matlab	TRSMm error
1	0.157297	0.157297	0.000000	0.157297	0.000000
2	0.152362	0.152362	0.000000	0.152362	0.000000
3	0.142492	0.142492	0.000000	0.142492	0.000000
4	0.127688	0.127688	0.000000	0.127688	0.000000
5	0.107948	0.107948	0.000000	0.107948	0.000000
6	0.083275	0.083275	0.000000	0.083275	0.000000
7	0.053665	0.053665	0.000000	0.053665	0.000000
8	0.019122	0.019122	0.000000	0.019122	0.000000

Table 2: Eigenvalues ($\times 10^{-3}$) for index of refraction$n^2(z) = 1 - 0.1cos(2\pi z/h)$.

TABLE 2: (x10e-3)

Mode	DSF analytic	TRSM fortran	TRSMf error	TRSM MC-Matlab	TRSMm error
1	0.165552	0.165543	0.000009	0.165553	0.000001
2	0.151019	0.151031	0.000012	0.151062	0.000043
3	0.139981	0.139976	0.000005	0.140015	0.000034
4	0.126508	0.126466	0.000042	0.126436	0.000072
5	0.107284	0.107263	0.000021	0.107259	0.000025
6	0.082841	0.082835	0.000006	0.082869	0.000028
7	0.053359	0.053364	0.000005	0.053436	0.000077
8	0.018893	0.018910	0.000017	0.019030	0.000137

Figure 3 - 10: Propagating modes: solid curves computed by Fortran program and +++ curves by PC-MATLAB.

Figure 11: Transmision loss versus range r:

$$TL = 10log_{10}[\|p(z,r)\|^2]$$

where

$$p(r,z) = \frac{i}{4}\sum_{n=0}^{\infty} \phi_n(z)\phi_n(z_0)H_0(ka_n r).$$

and source depth $z_0 = 500$, receiver depth $z = 1000$, $200 \le r \le 20000$. The dotted curve is for a homogeneous ocean $n(z) = 1$, and the solid curve is for the stratified ocean $n(z) = 1 - 0.1cos(2\pi z/h)$. We will consider an inverse problem to reconstruct the index of refraction by using this data.

Figure 12: Transmision loss versus range r: where source depth $z_0 =$ 500, receiver depth $z = 1000$, $500 \le r \le 50000$.

Figure 13: Transmision loss versus range r : where source depth $z_0 =$ 500, receiver depth z=1000, $r_0 = 10$, $1000 \le r \le 100000$.

Figure 14: Finite difference scheme.

Example 2 This example is an idealized ocean model for an ocean sound channel with its axis at one-fifth the depth of the ocean. The index of refraction is

$$n^2(z) = 1 + 0.1 \left[sin(\frac{5\pi}{4h}z) - \frac{2\sqrt{2}}{5\pi} \right]$$

where the depth of ocean $h = 5000$, and $k = 8\pi/5000$.

Figure 15: The transmutation kernel $K(z, s)$ for example 2.

Figure 16: The eigenvalues shown bracketed by two os, which are the zeros of

$$cos(\lambda) + \int_h^0 K(0, s) cos[\lambda(1 - \frac{s}{h})]ds = 0.$$

Table 3: Unperturbed eigenvalues ($\times 10^{-4}$) for example 1. The index of refraction $n^2(z) = 1$.

TABLE 3: (x10e-4)

Mode	DSF analytic	TRSM fortran	TRSMf error	TRSM MC-Matlab	TRSMm error
1	0.251675	0.251675	0.000000	0.251675	0.000000
2	0.243779	0.243779	0.000000	0.243779	0.000000
3	0.227988	0.227988	0.000000	0.227988	0.000000
4	0.204301	0.204301	0.000000	0.204301	0.000000
5	0.172718	0.172718	0.000000	0.172718	0.000000
6	0.133240	0.133240	0.000000	0.133240	0.000000
7	0.085866	0.085656	0.000000	0.085656	0.000000
8	0.030596	0.030596	0.000000	0.030596	0.000000

Table 4: Eigenvalues ($\times 10^{-4}$) for index of refraction$n^2(z) = 1{+}0.1 sin(5\pi z/4h + \pi/4) - 0.2\sqrt{2}/5\pi$.

TABLE 4: (x10e-4)

Mode	DSF analytic	TRSM fortran	TRSMf error	TRSM MC-Matlab	TRSMm error
1	0.260430	0.260608	0.000178	0.260870	0.000440
2	0.237756	0.238109	0.000353	0.238656	0.000900
3	0.221614	0.221957	0.000343	0.222472	0.000858
4	0.202254	0.202403	0.000149	0.202586	0.000332
5	0.171646	0.171741	0.000095	0.171872	0.000226
6	0.132547	0.132620	0.000073	0.132760	0.000213
7	0.085379	0.085445	0.000066	0.085621	0.000242
8	0.030234	0.030303	0.000069	0.030540	0.000306

Figure 17 - 24: Propagating modes: solid curves computed by Fortran program and +++ curves by PC-MATLAB.

Figure 25: Transmision loss versus range r : where source depth $z_0 =$ 500, receiver depth z=1000, $r_0 = 10$, $200 \le r \le 20000$.

Figure 26: Transmision loss versus range r : where source depth $z_0 =$ 500, receiver depth z=1000, $r_0 = 10$, $500 \le r \le 50000$.

Figure 27: Transmision loss versus range r : where source depth $z_0 =$ 500, receiver depth z=1000, $r_0 = 10$, $1000 \le r \le 100000$.

Figure 28: Finite difference scheme.

References

[1] Ahluwalia, D. and Keller, J.; "Exact and asymptotic representations of the sound field in a stratified ocean," *Wave Propagation and Underwater Acoustics*, Leture Notes in Physics 70, Springer, Berlin (1977)

[2] Aziz, A. K. and Hubbard, B.E.; "Bounds on the truncation error by finite differences for the Goursat problem", (1964)

[3] Duston, M., Gilbert, R. P., Verma, G. H. and Wood, D. H.; " Direct generation of normal modes by transmution theory, " *Computational Acoustics: Algorithms and Applications, Vol.2.* (1987) 389-402.

[4] Gilbert, R. P. and Wood, D. H.; "A transmutation approach to underwater sound propagation," *Wave Motion 8* (1986) 383-397.

[5] Gilbert, R. P. and Xu, Y.; "Starting fields and far fields in ocean acoustics", *Wave Motion*, to appear, (1989).

[6] Gilbert, R. P. and Xu, Yongzhi; "Dense sets and the projection theorem for acoustic harmonic waves in homogeneous finite depth ocean", preprint, (1988).

[7] Gilbert, R. P. and Xu, Yongzhi; "The propagation problem and far-field patterns in a stratified finite depth ocean", preprint, (1988).

[8] Gilbert, R. P. , Xu, Yongzhi and Thejll, P.; "An approximation scheme for three-dimensional scattered wave and its propagating far-field pattern in a finite depth ocean", (1988).

[9] Gilbert, R. P. , Xu, Yongzhi and Wood, D.H.; "Construction of approximation to acoustic Green's functions for nonhomogeneous ocean

using transmutations" , *Wave Motion 10* (1988) 285-297.

[10] Xu,Yongzhi; "An injective far-field pattern operator and inverse scattering problem in a finite depth ocean", pre-print, (1988)

[11] *PC-MATLAB USER'S GUIDE,* Mathworks, South Natick, MA, (1986).

[12] Jensen, F.B. and Ferle, M.C.; "SNAP: The SACLANTCEN normal-mode aco2stic propagation model," SACLANCEN Memorandum SM-121, SACLANT ASW Research Center, La Spezia, Italy (15 January 1979).

[13] Robinson, E. R. and Wood, D. H.; "Generating starting fields for parabolic equations," *J. Acoust. Soc. Amer.* 84 (1988) 1794-1801.

[14] Gilbert, R.P., Wood, D.H. and Xu, Y.; "Underwater acoustics for Submersibles" , Proceedings EEZ Resources: Technology Assessment Conference, Ocean Technology Congress, Jan. 22-26, 1989, Honolulu, Hawaii, 8-52 to 8-61.

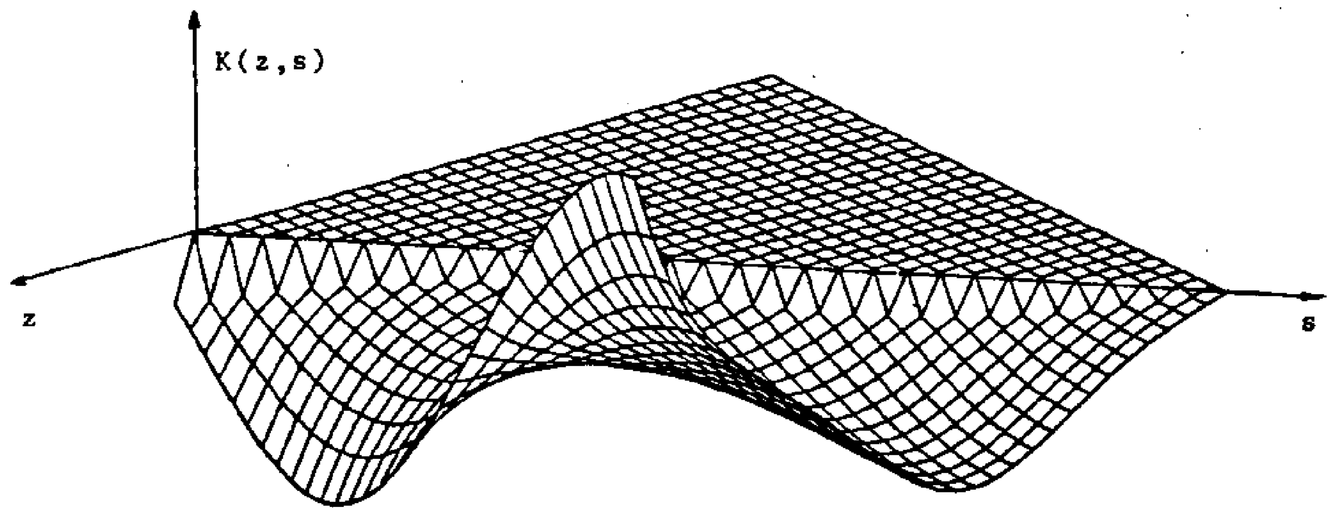

Figure 1

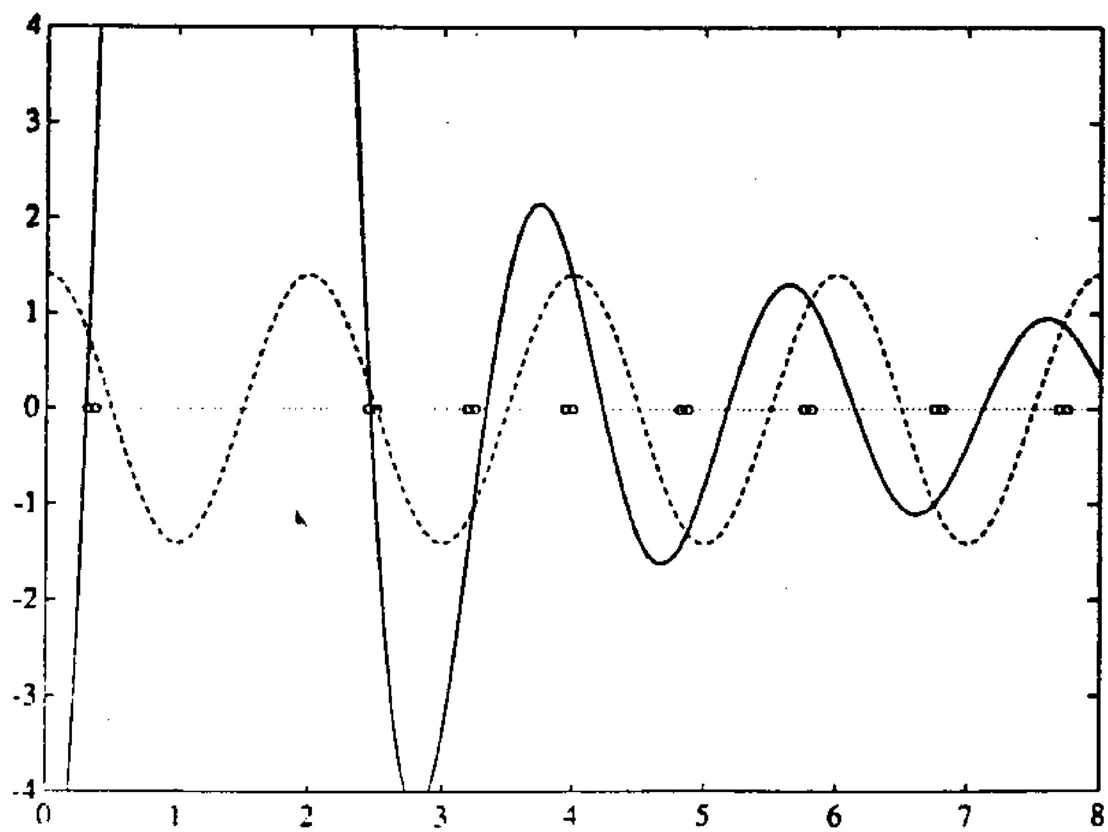

Figure 2

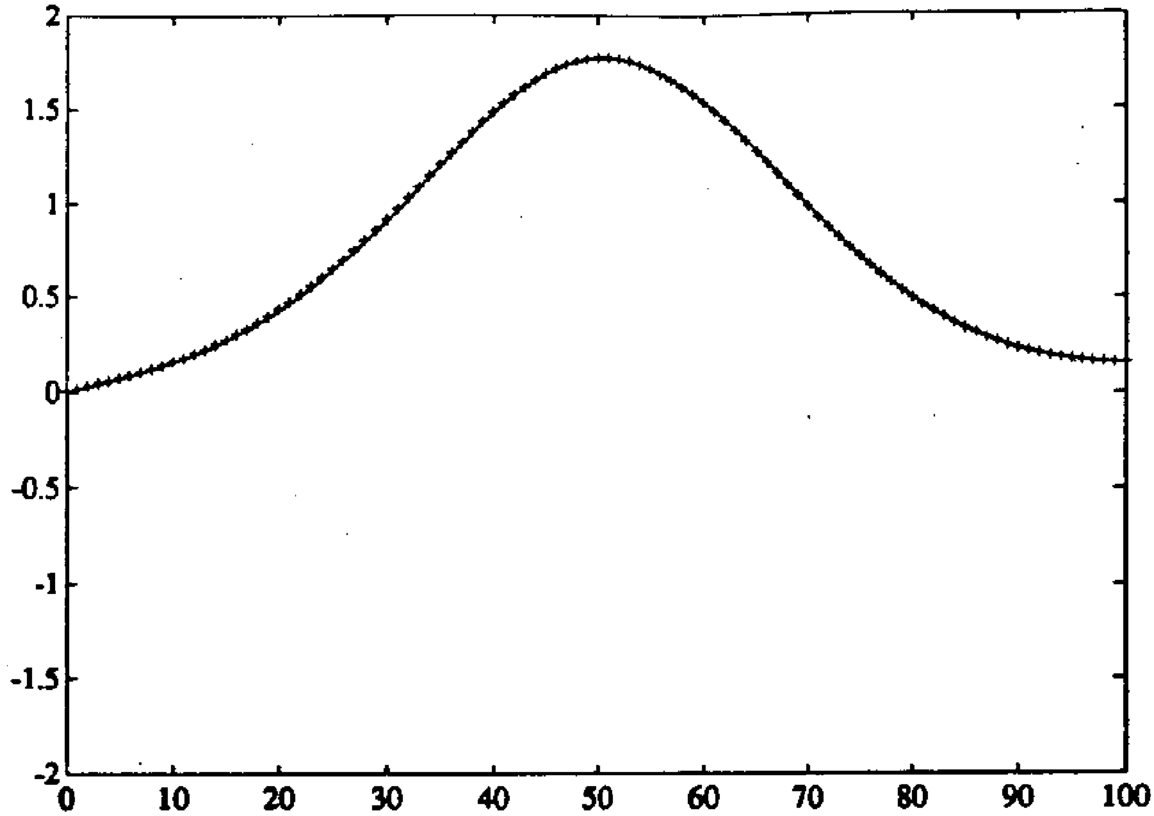

Figure 3

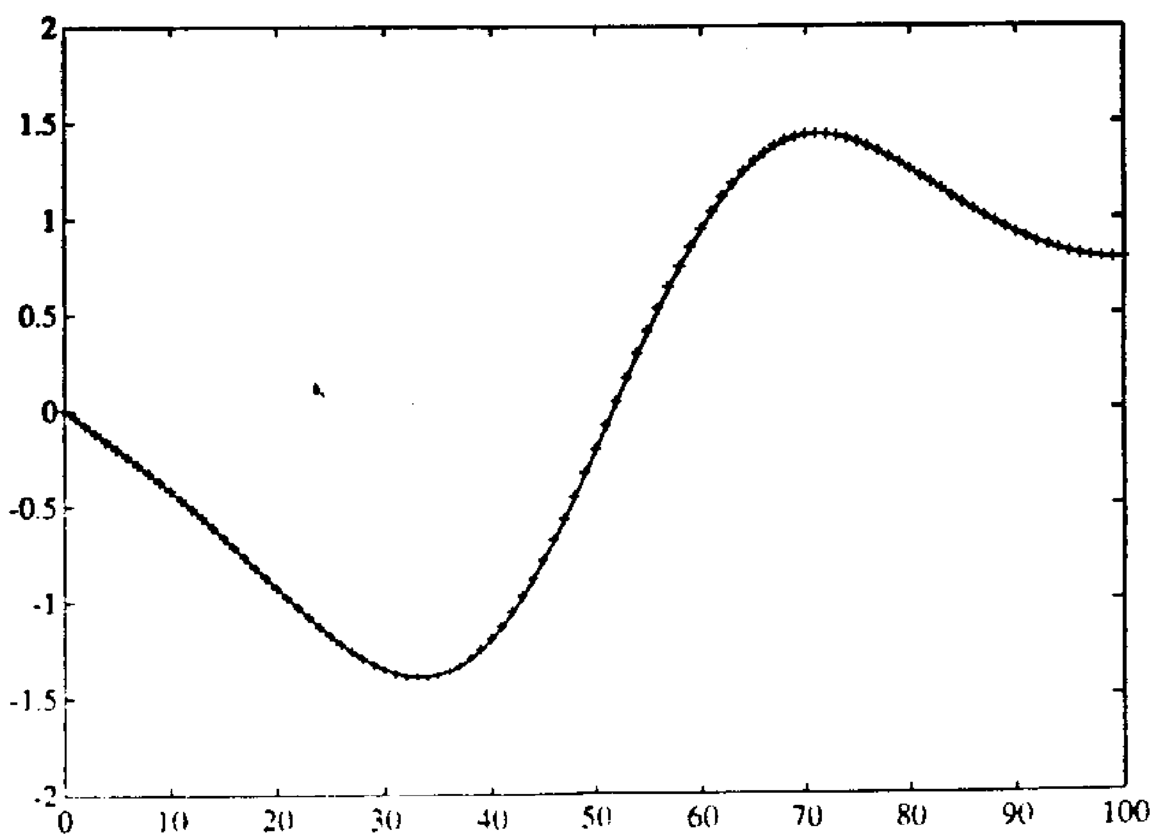

Figure 4

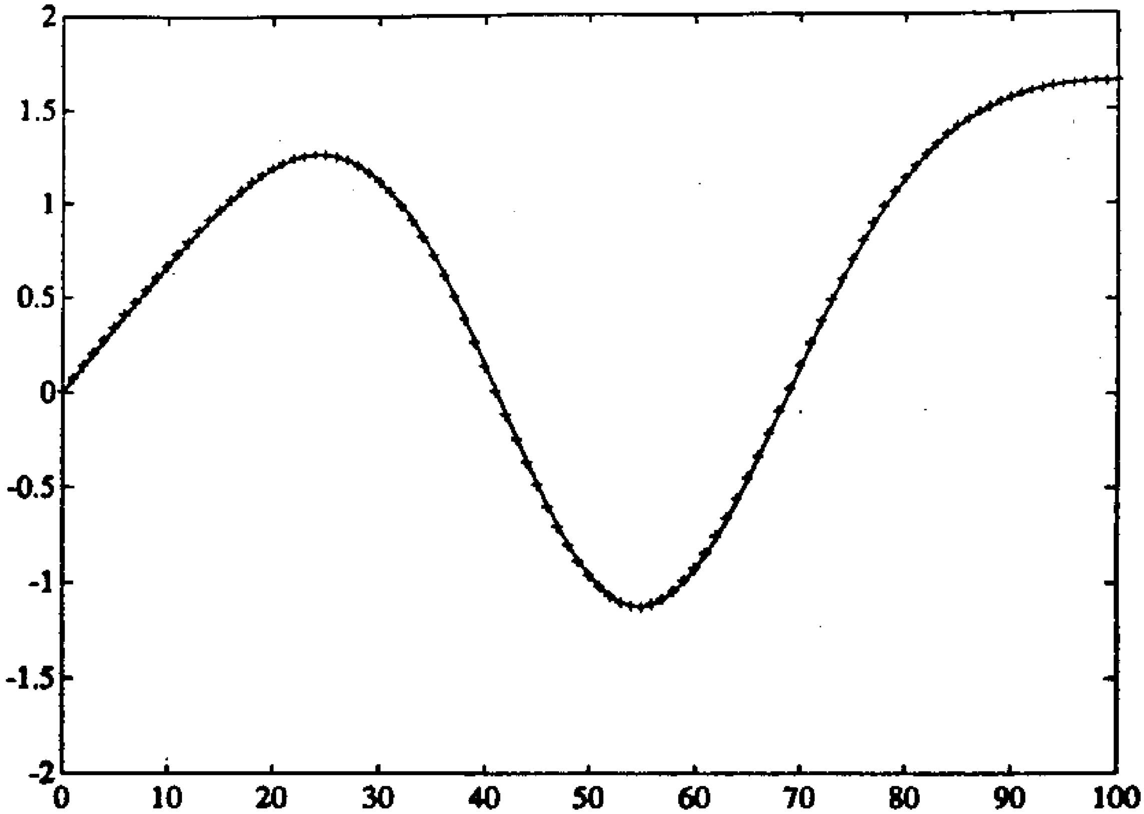

Figure 5

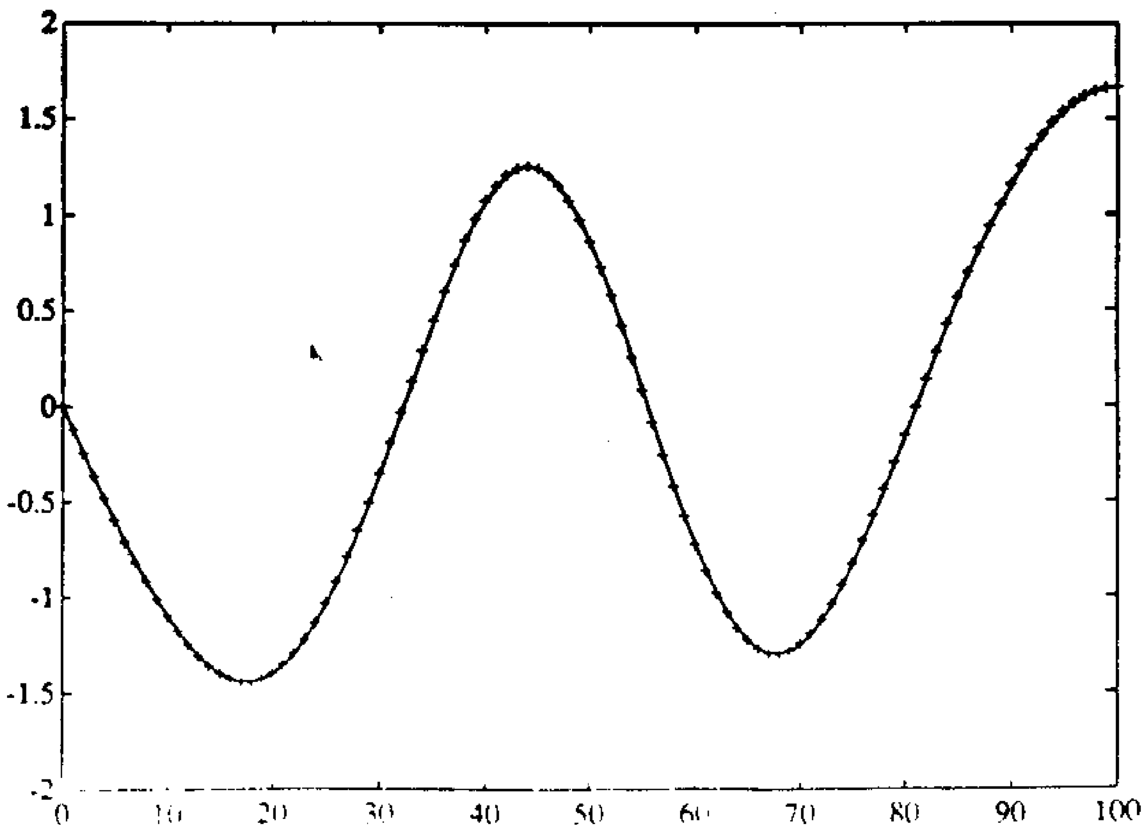

Figure 6

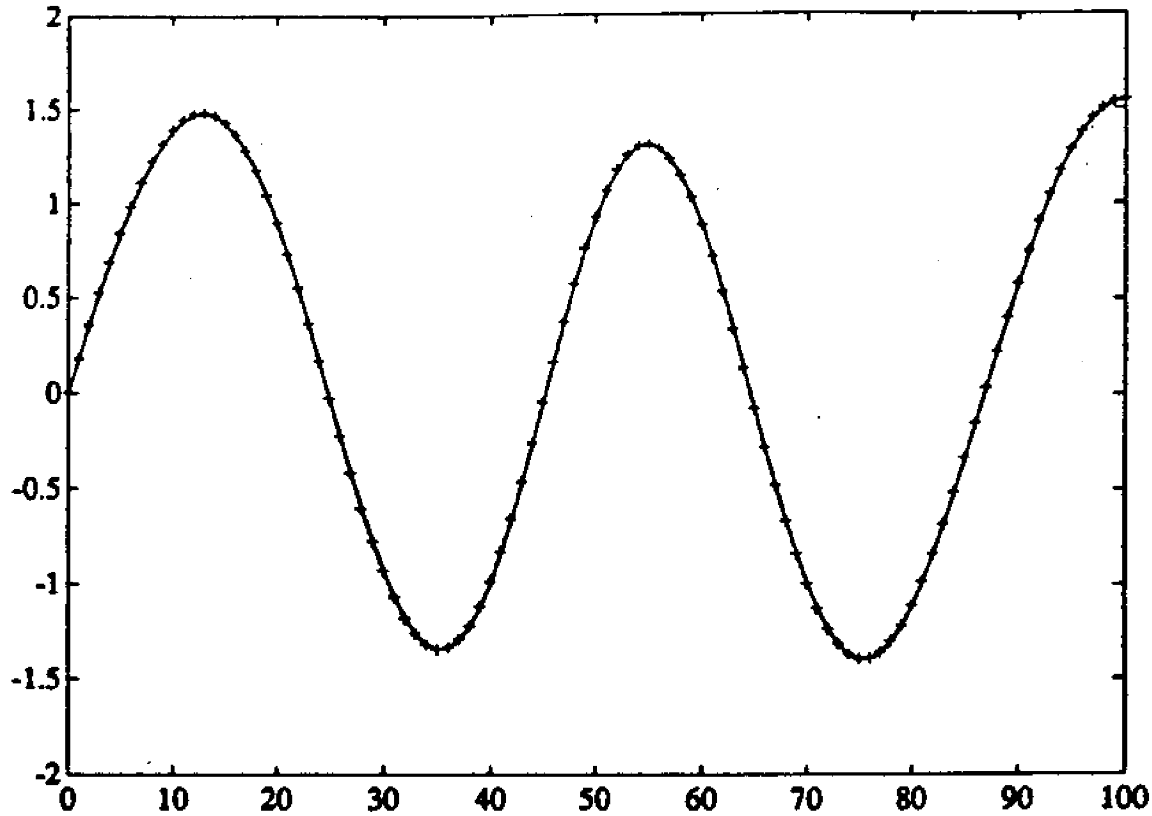

Figure 7

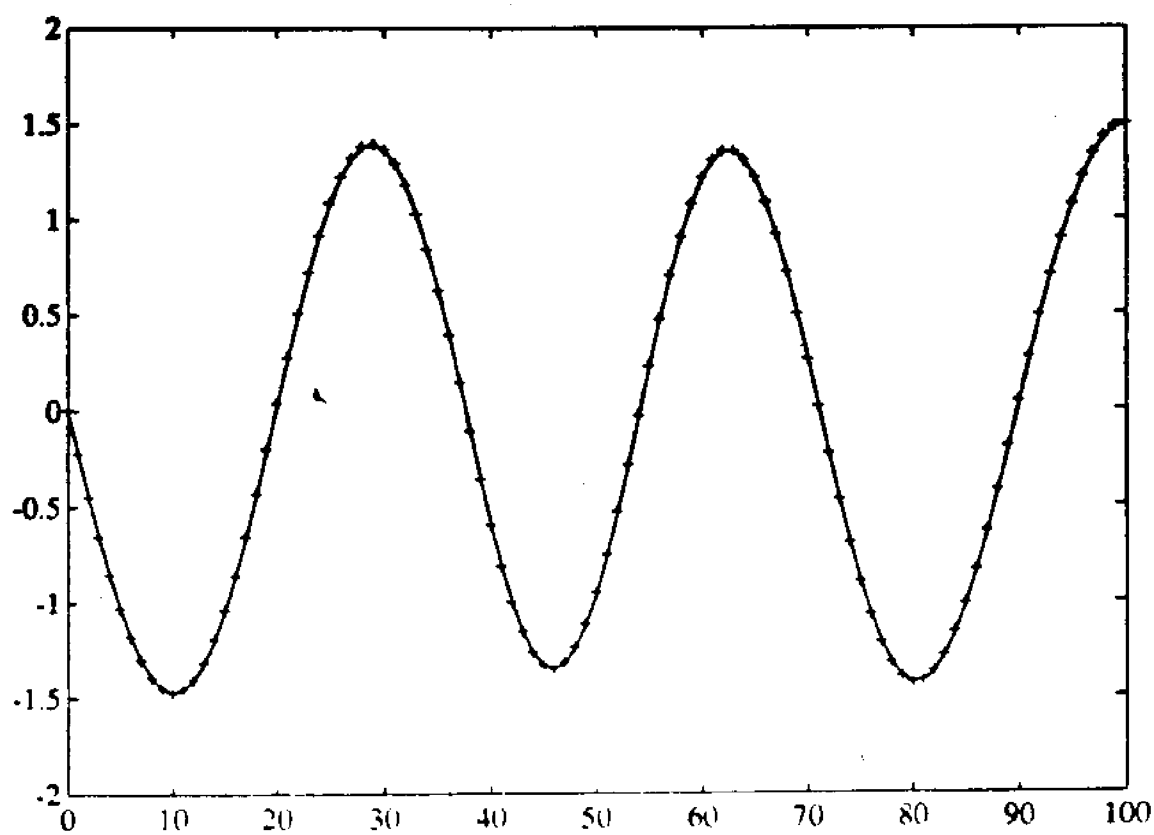

Figure 8

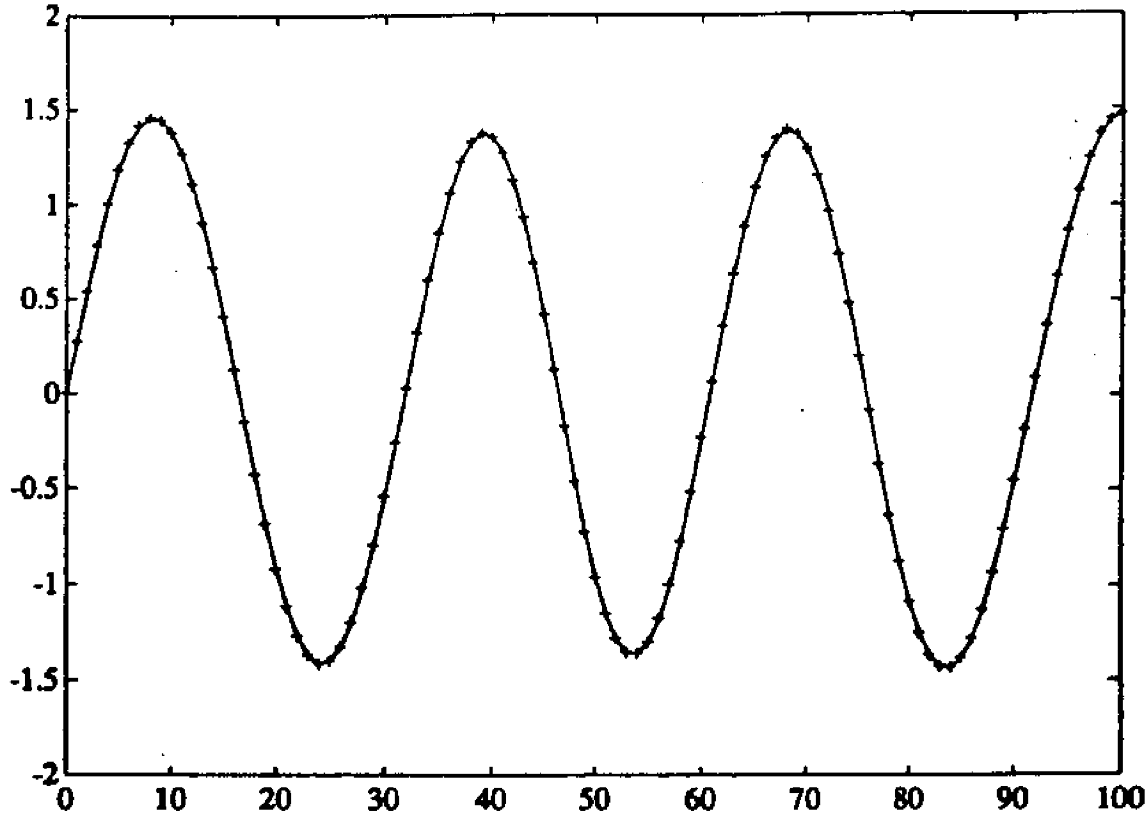

Figure 9

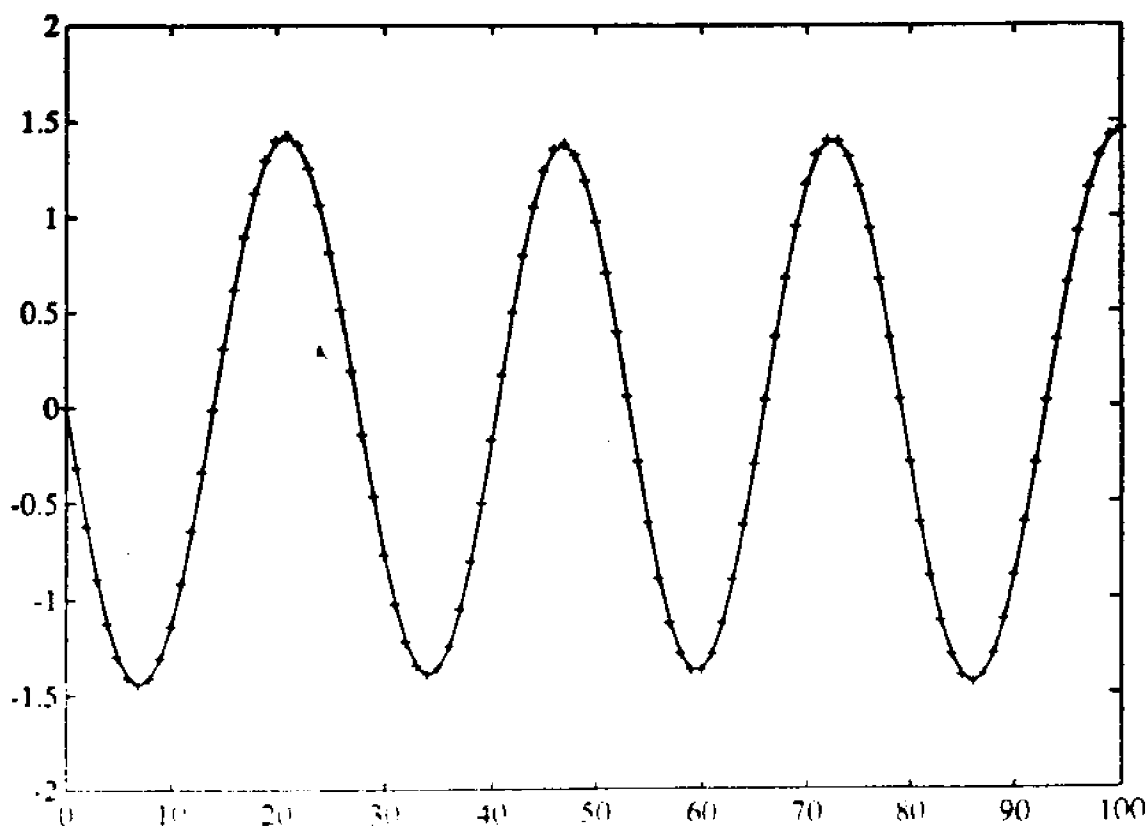

Figure 10

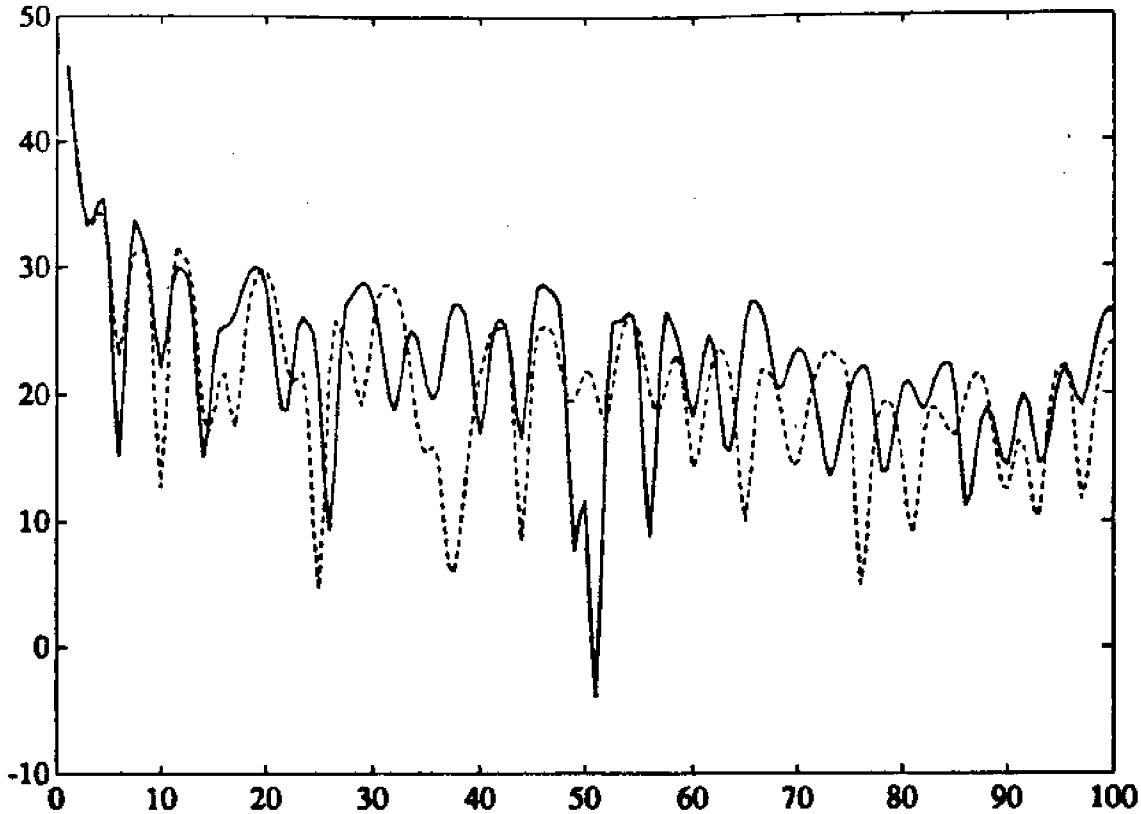

Figure 11

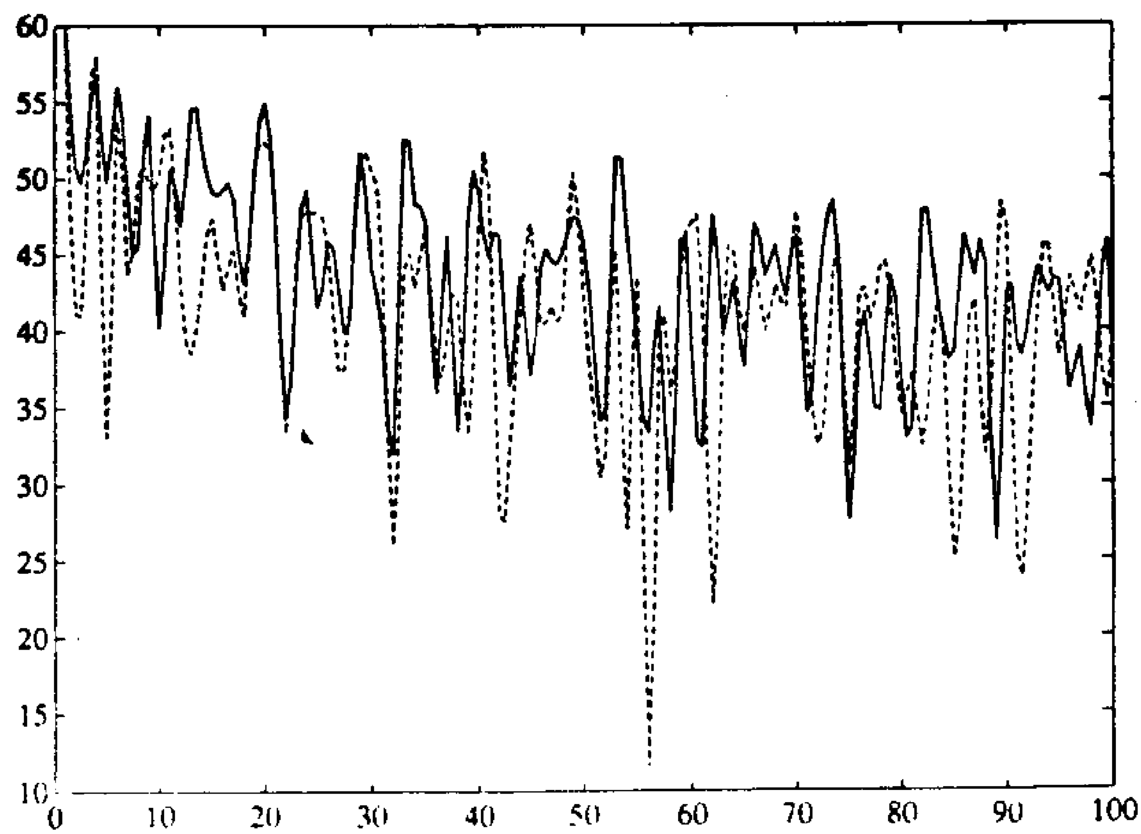

Figure 12

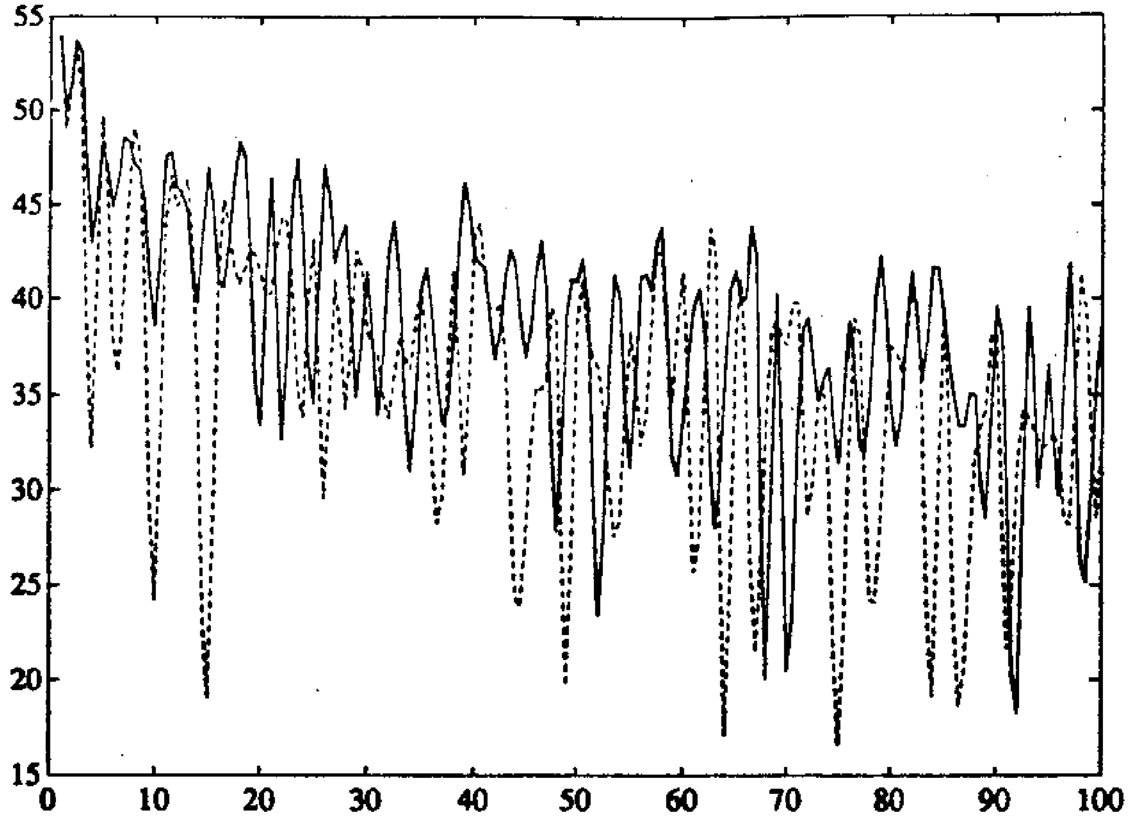

Figure 13

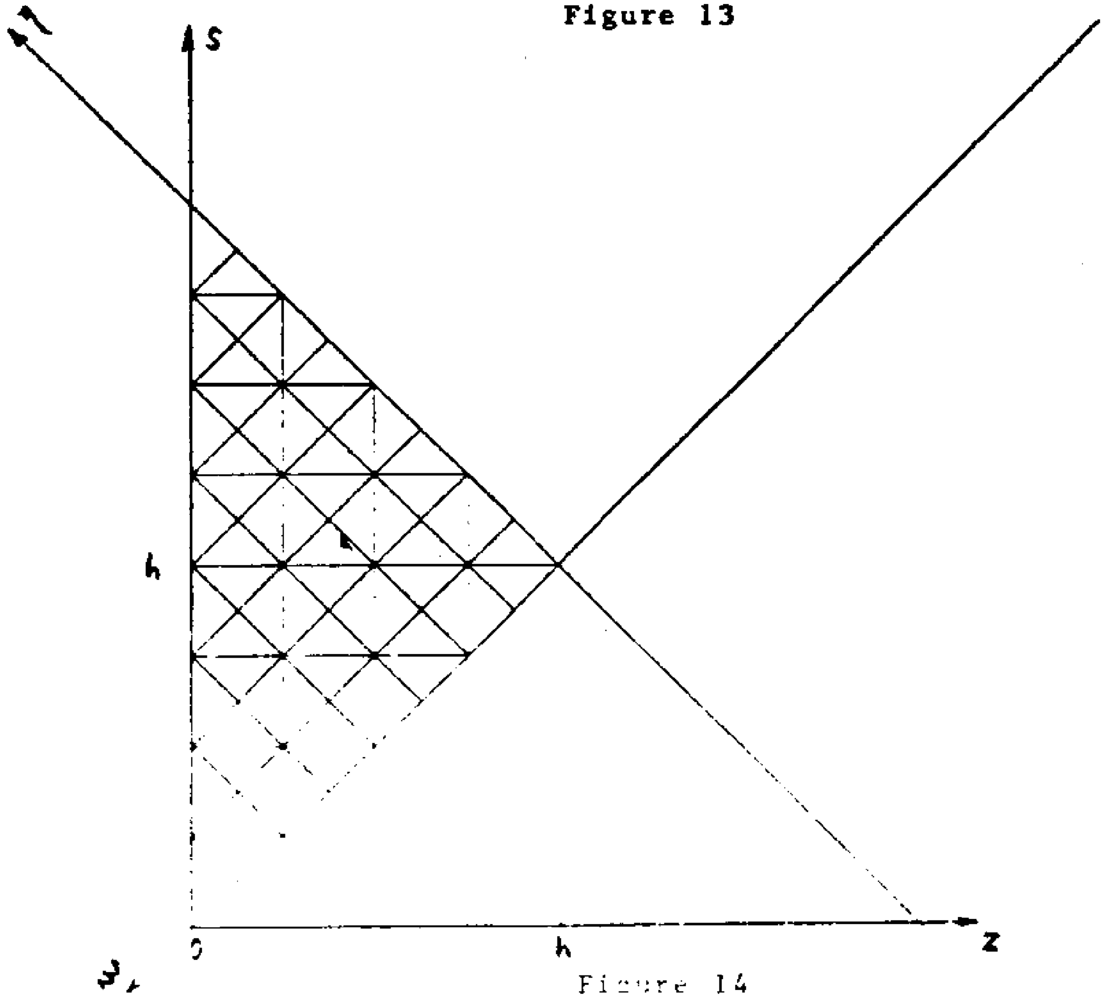

Figure 14

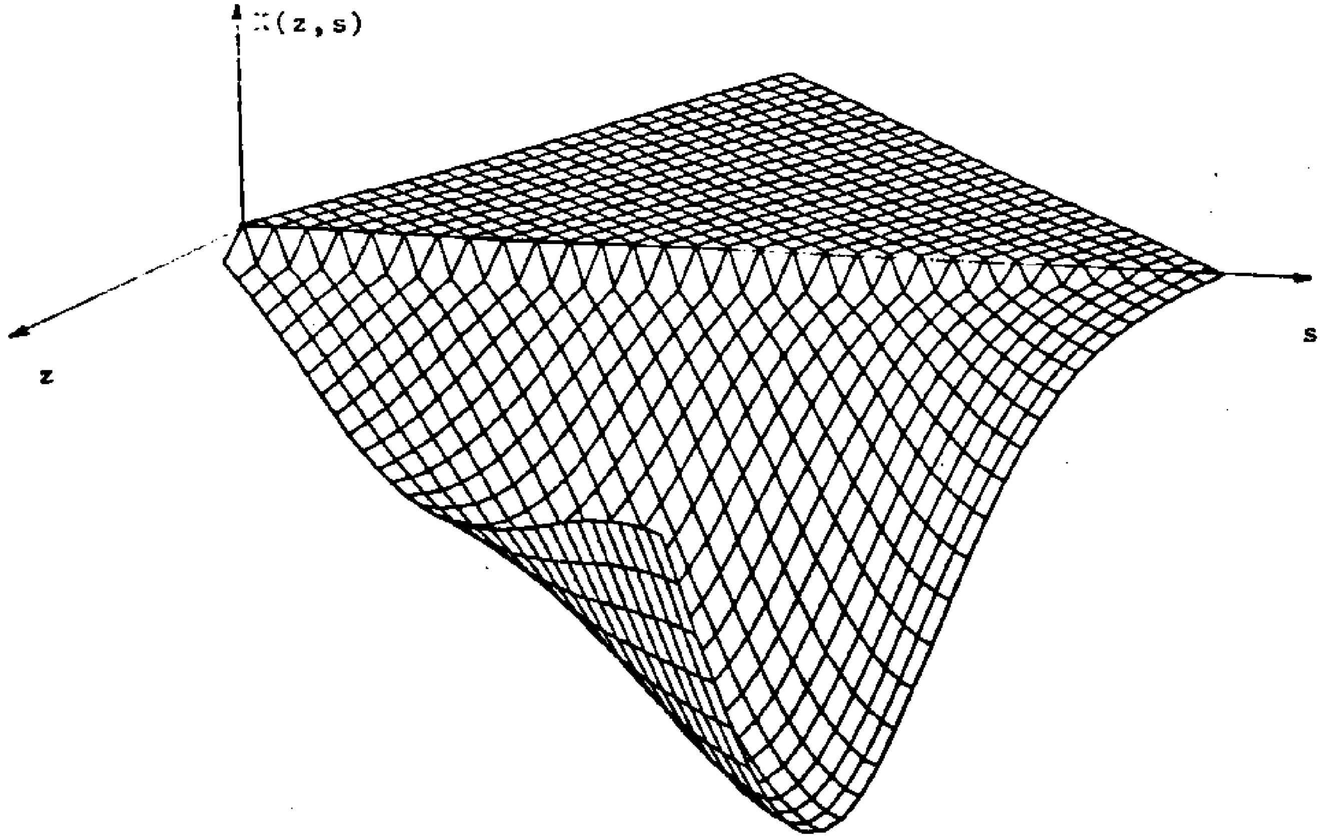

Figure 15

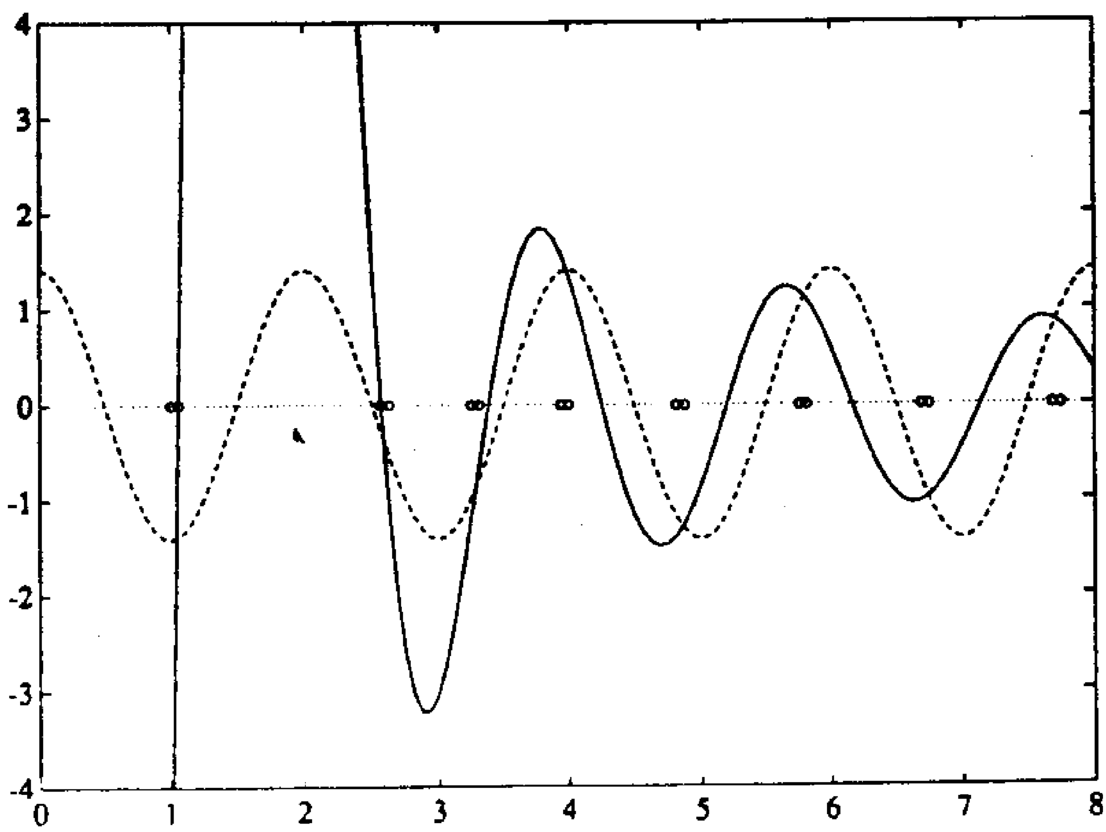

Figure 16

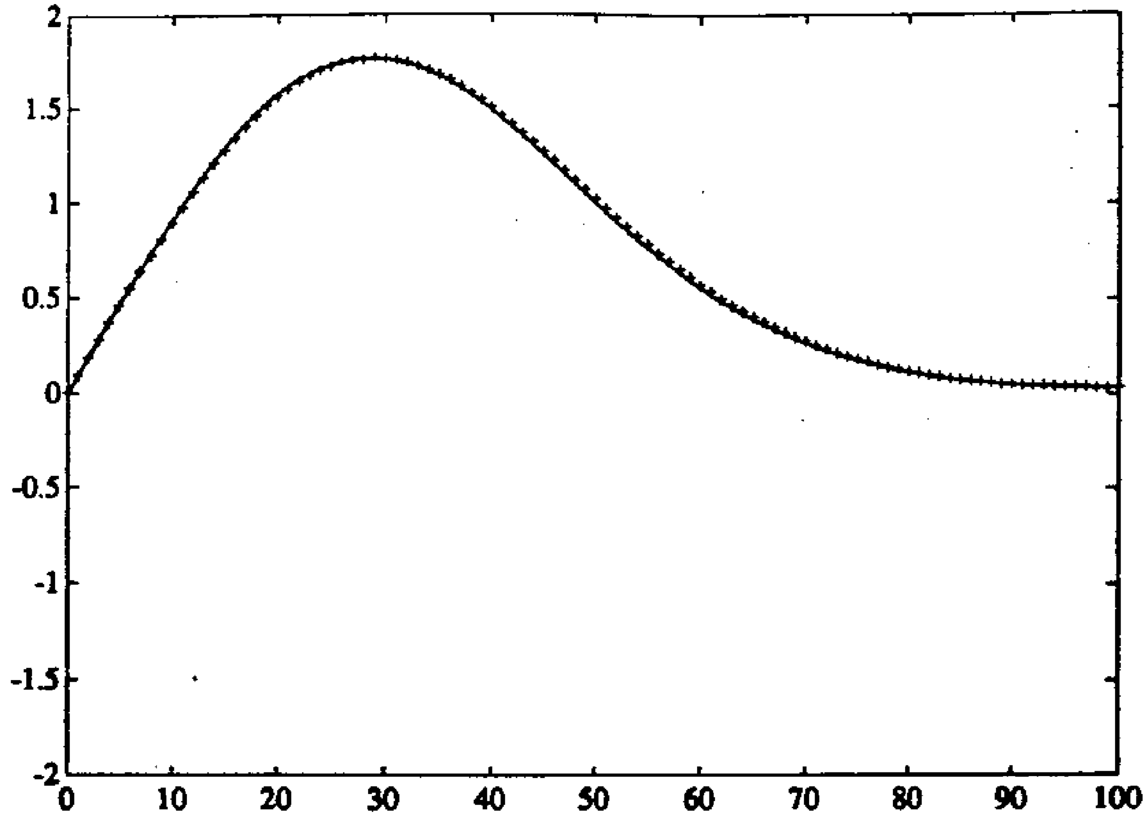

Figure 17

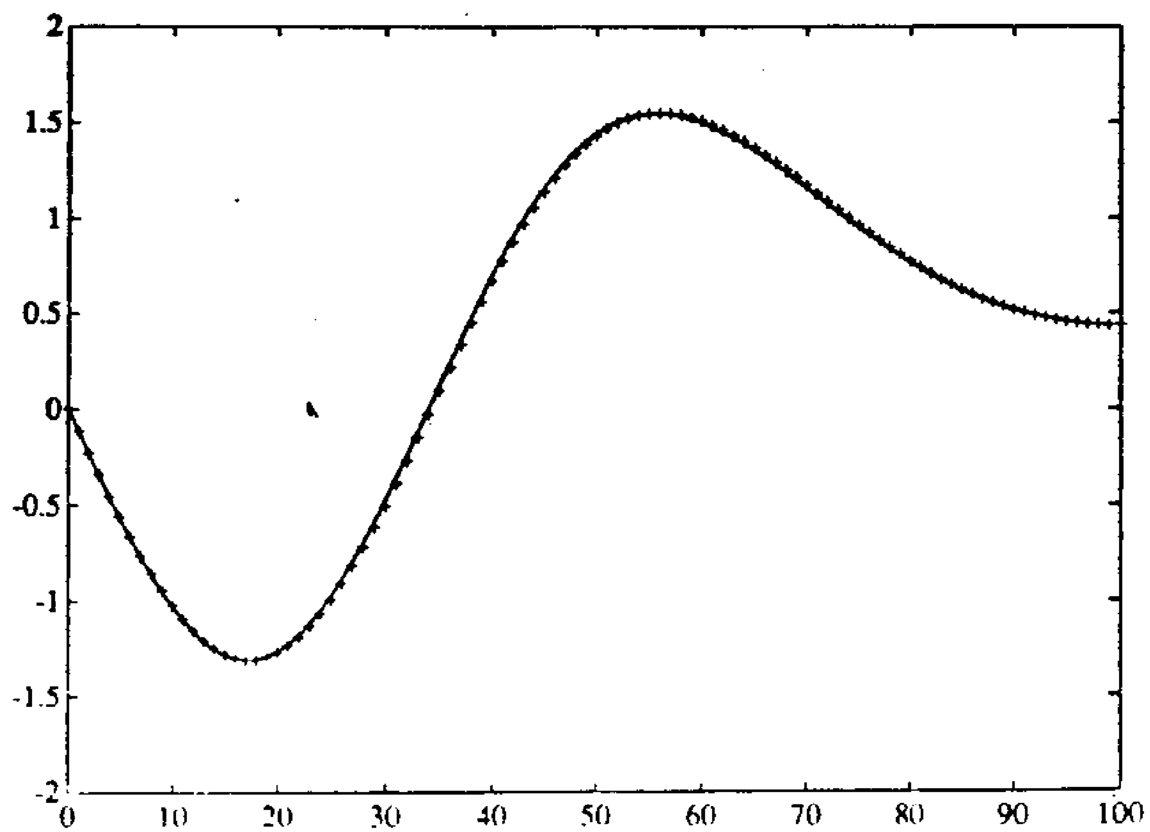

Figure 18

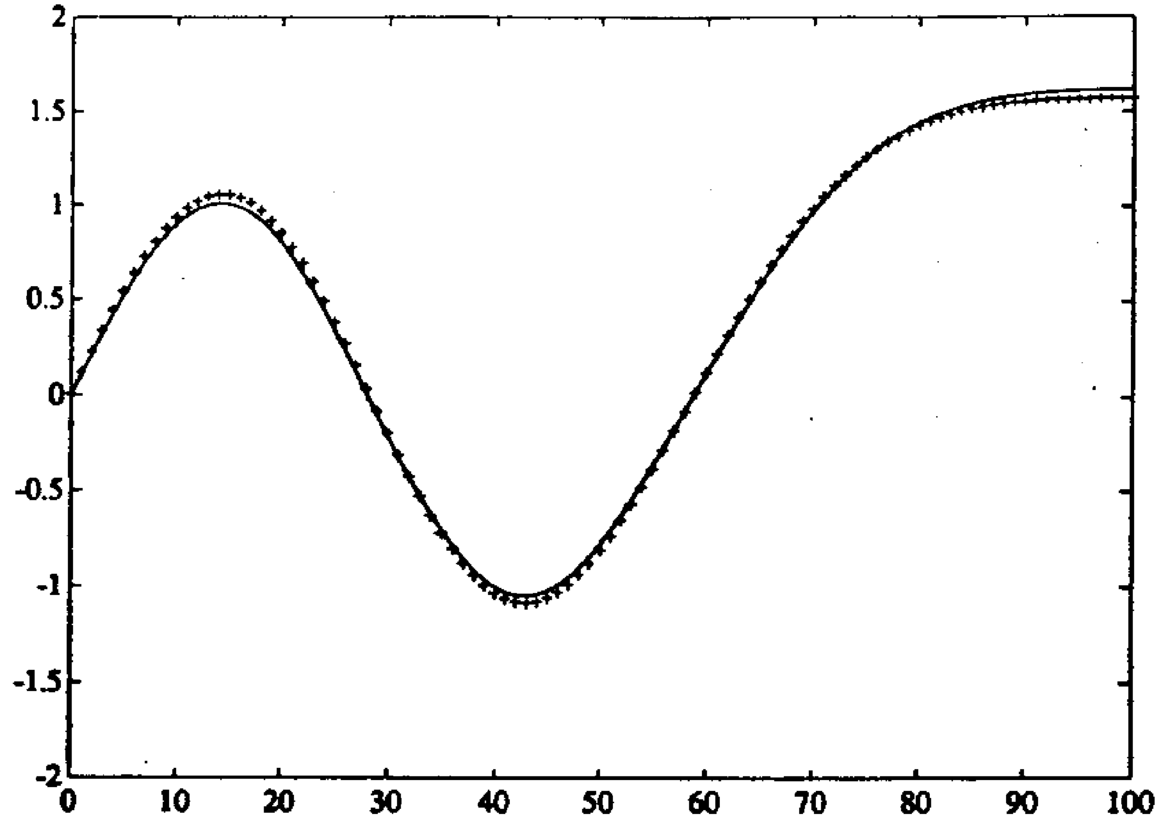

Figure 19

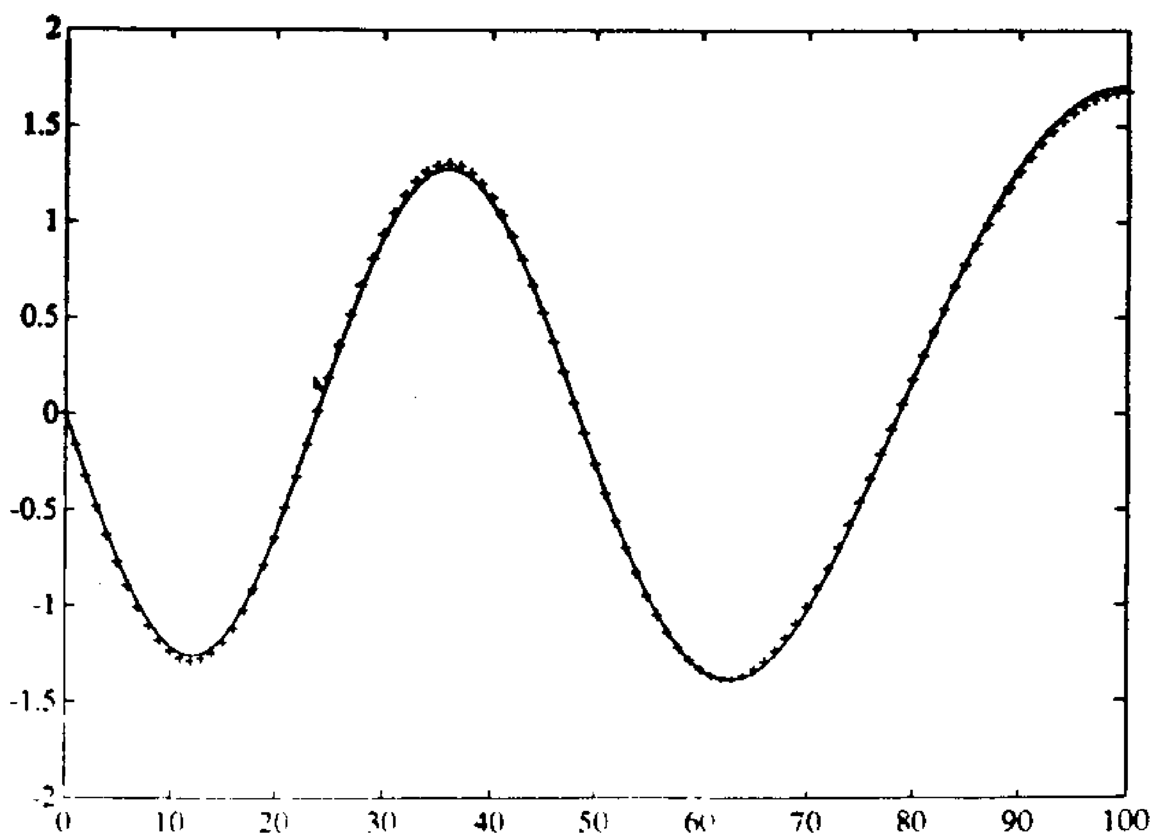

Figure 20

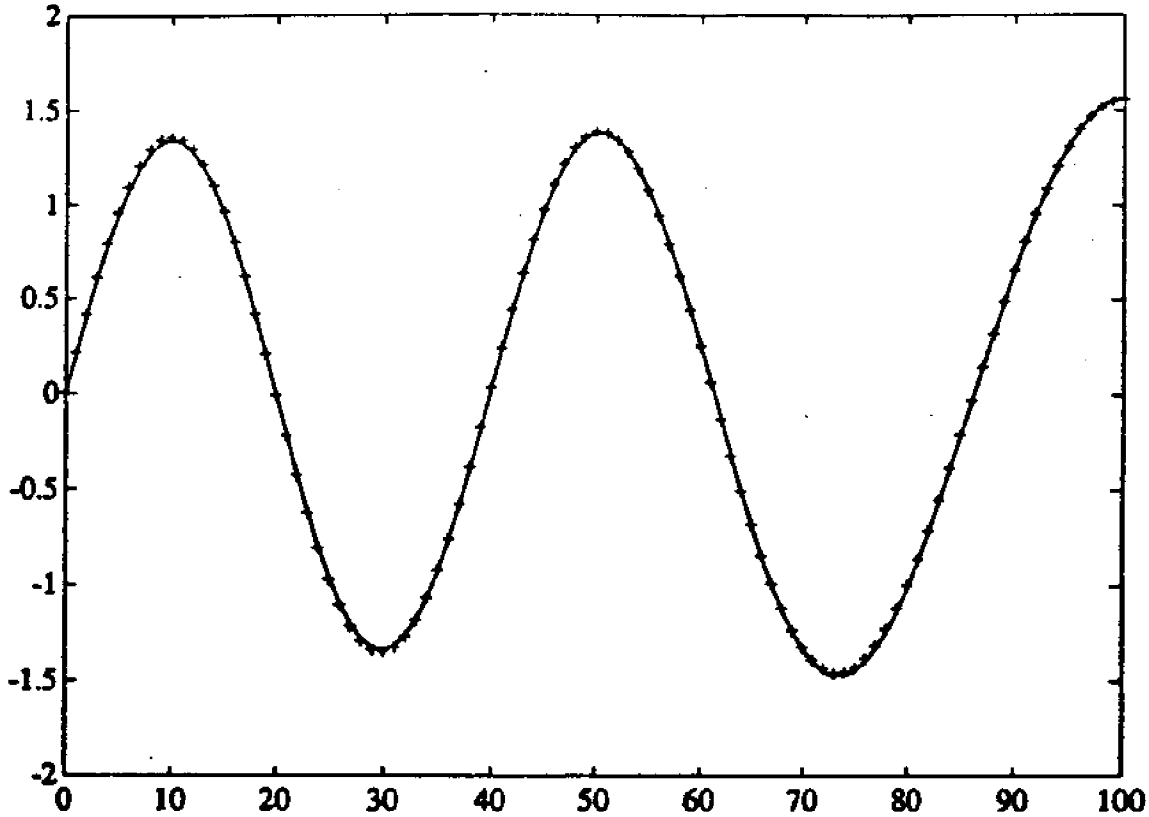

Figure 21

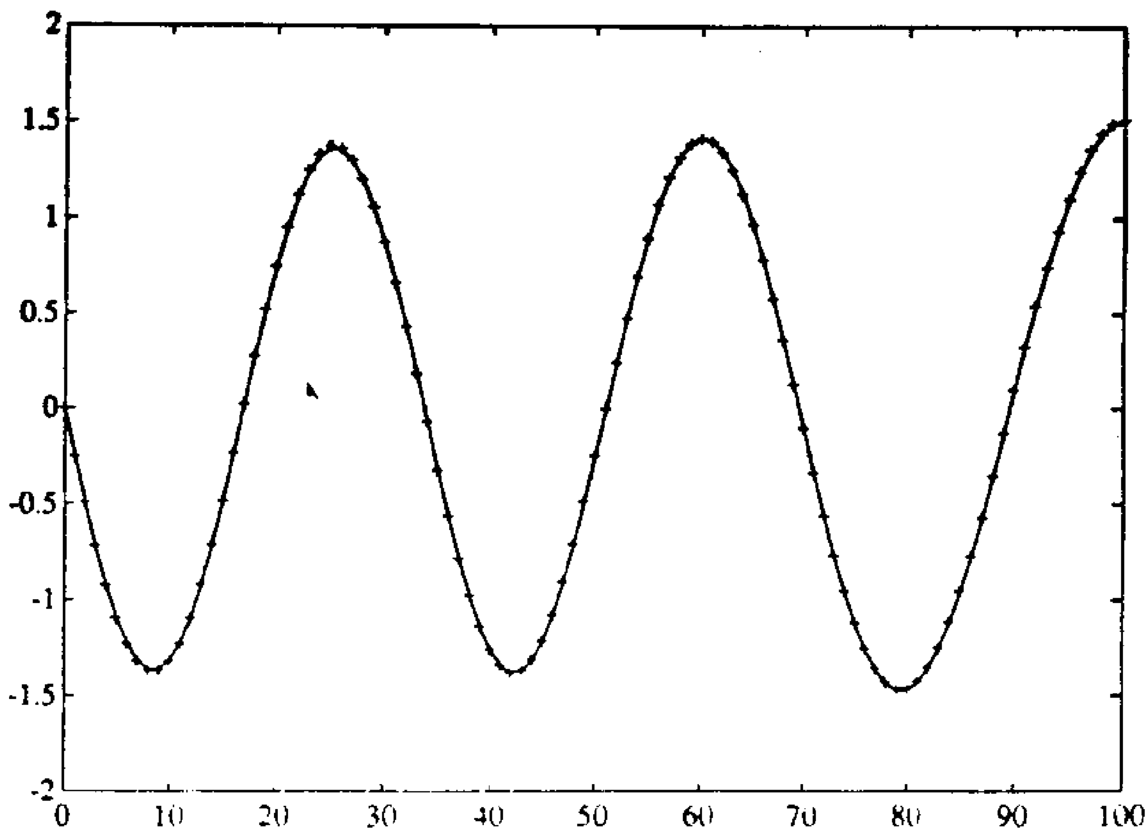

Figure 22

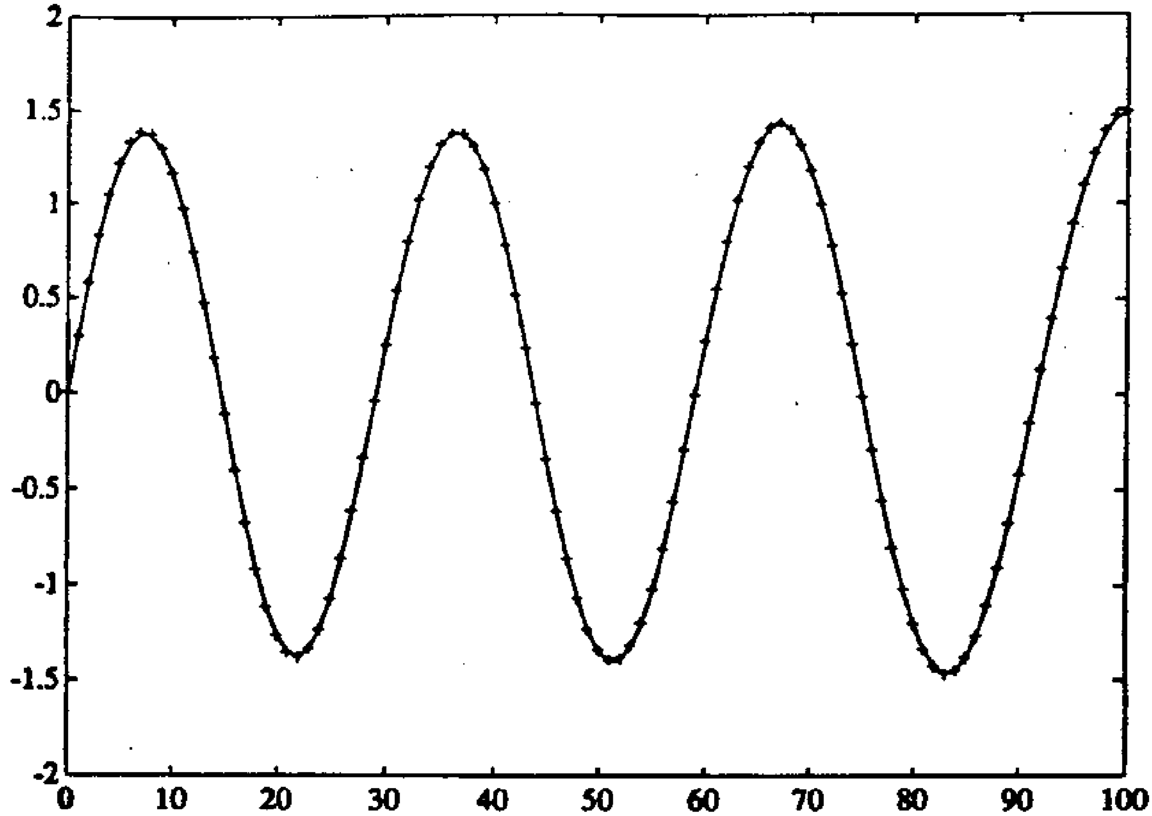

Figure 23

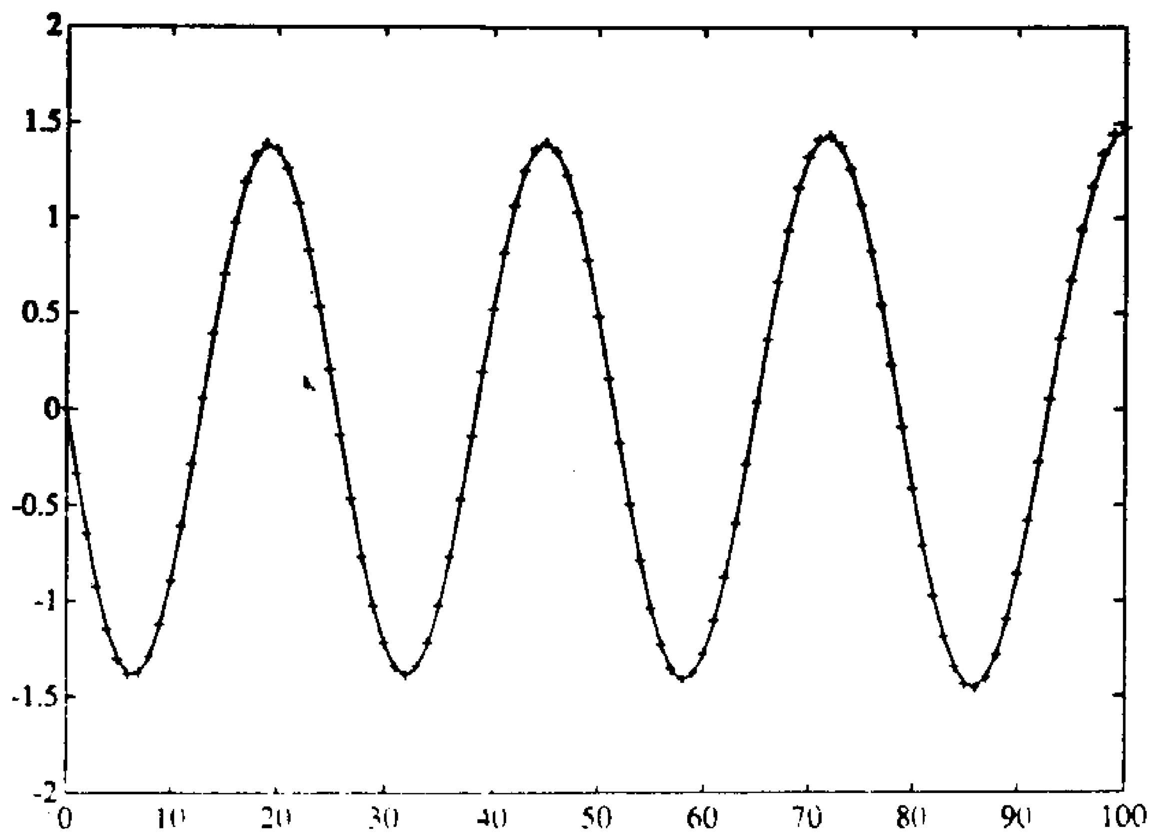

Figure 24

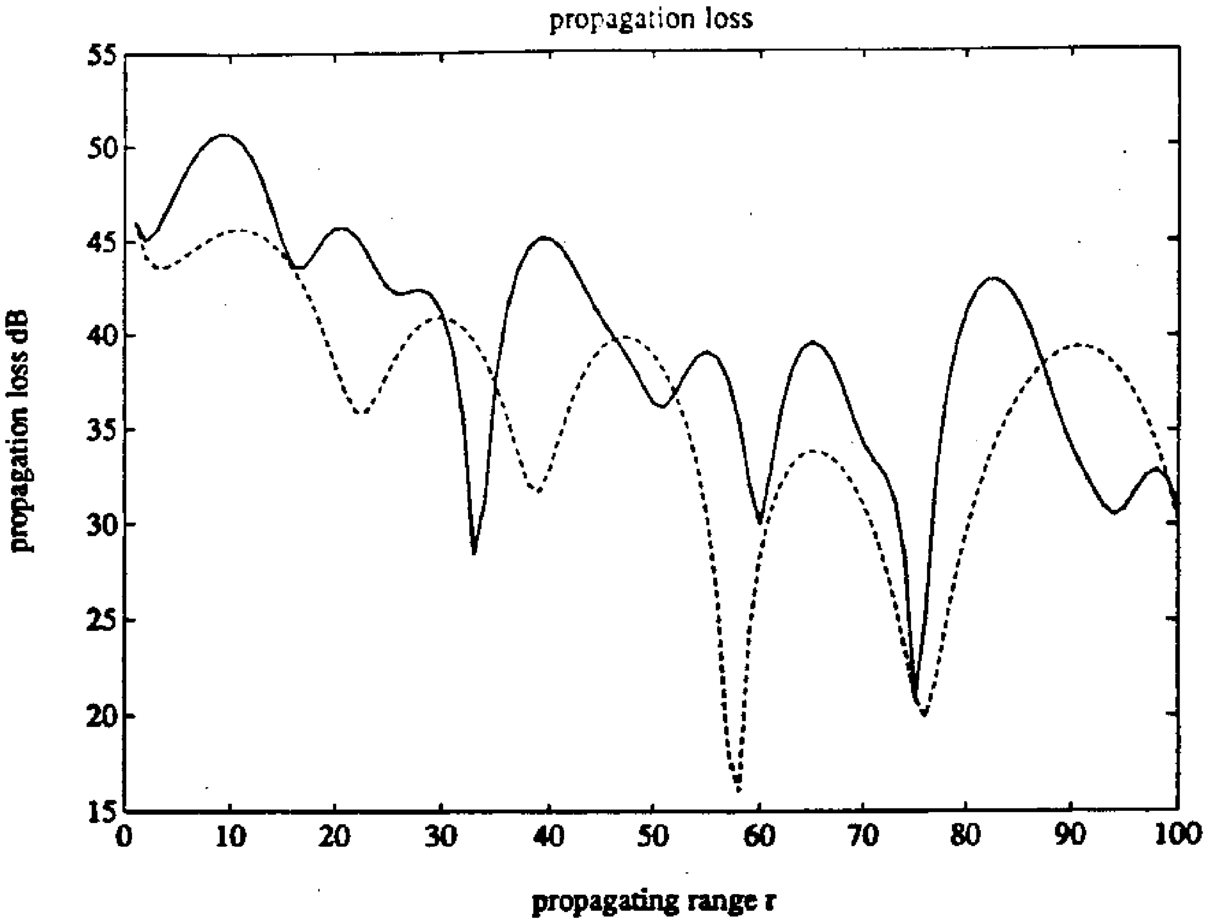

Figure 25

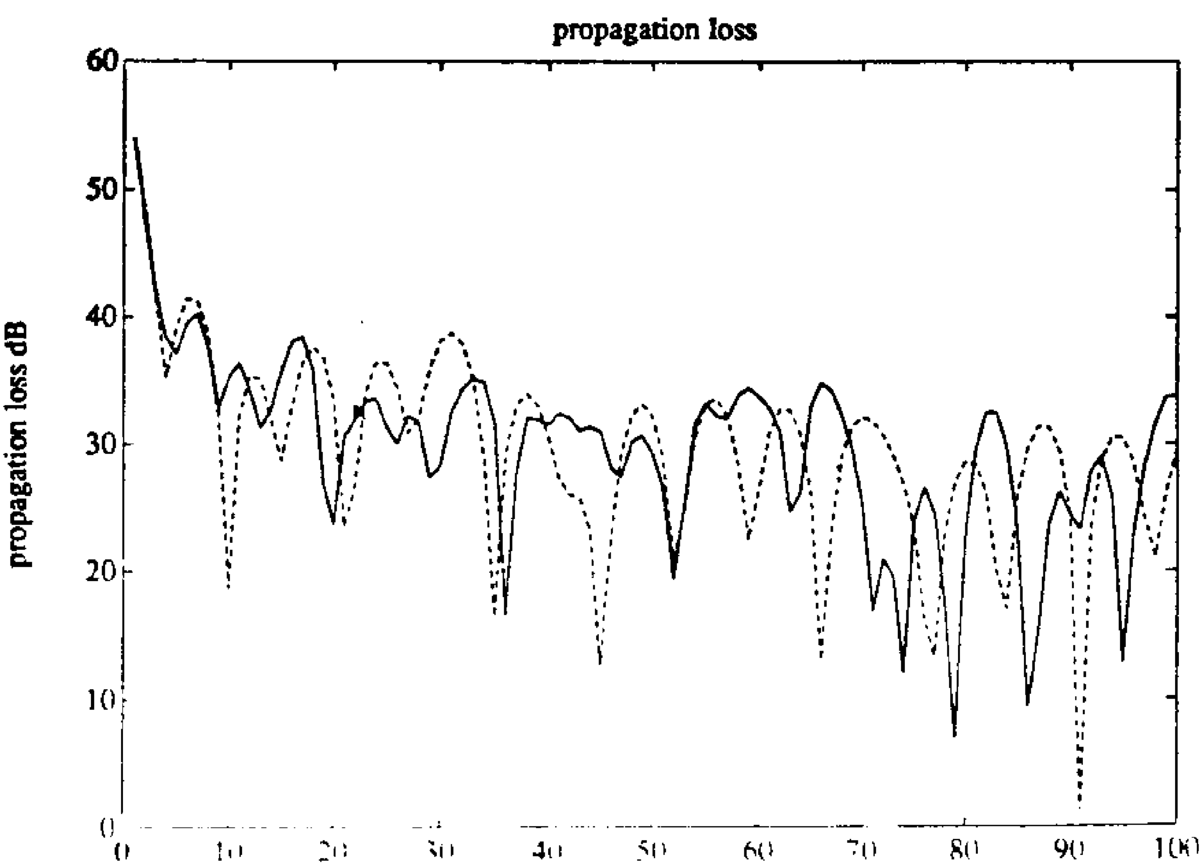

Figure 26

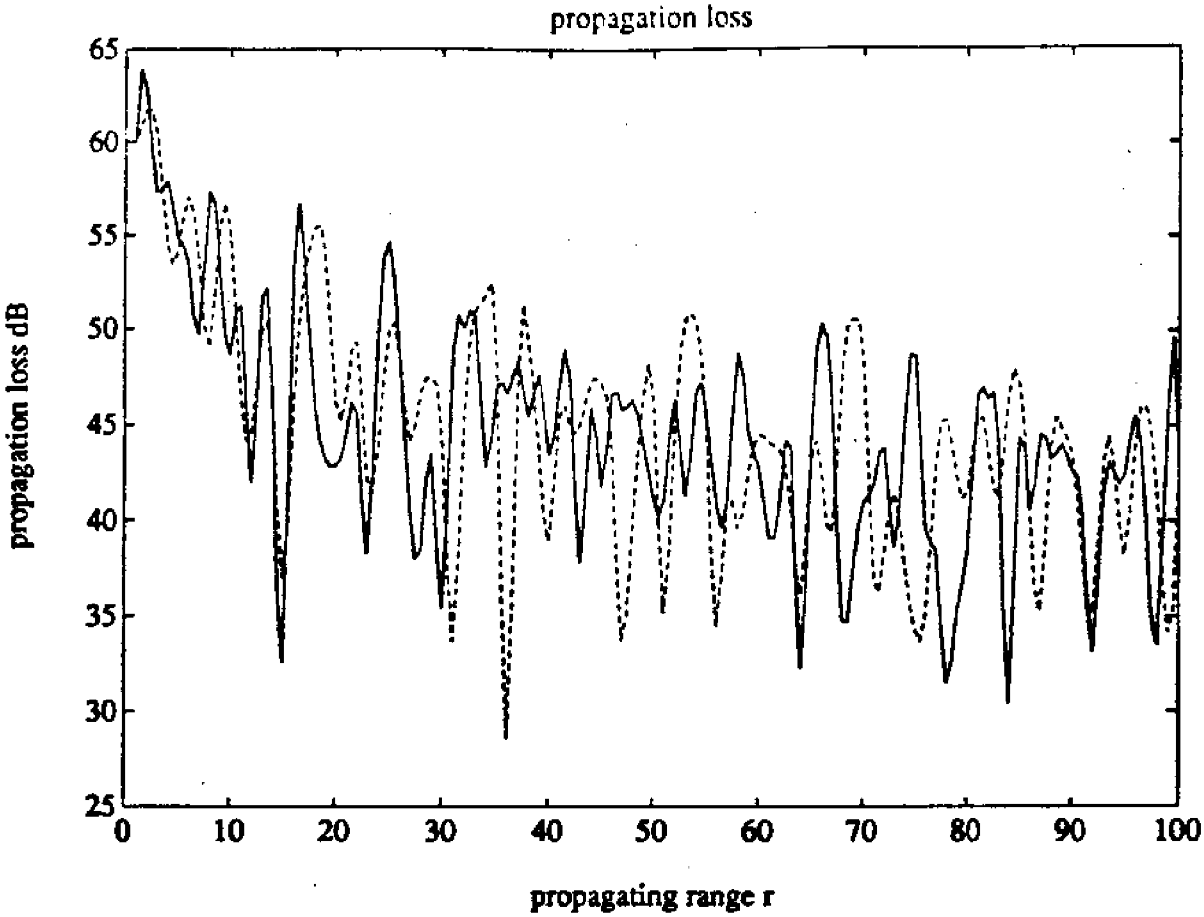

Figure 27

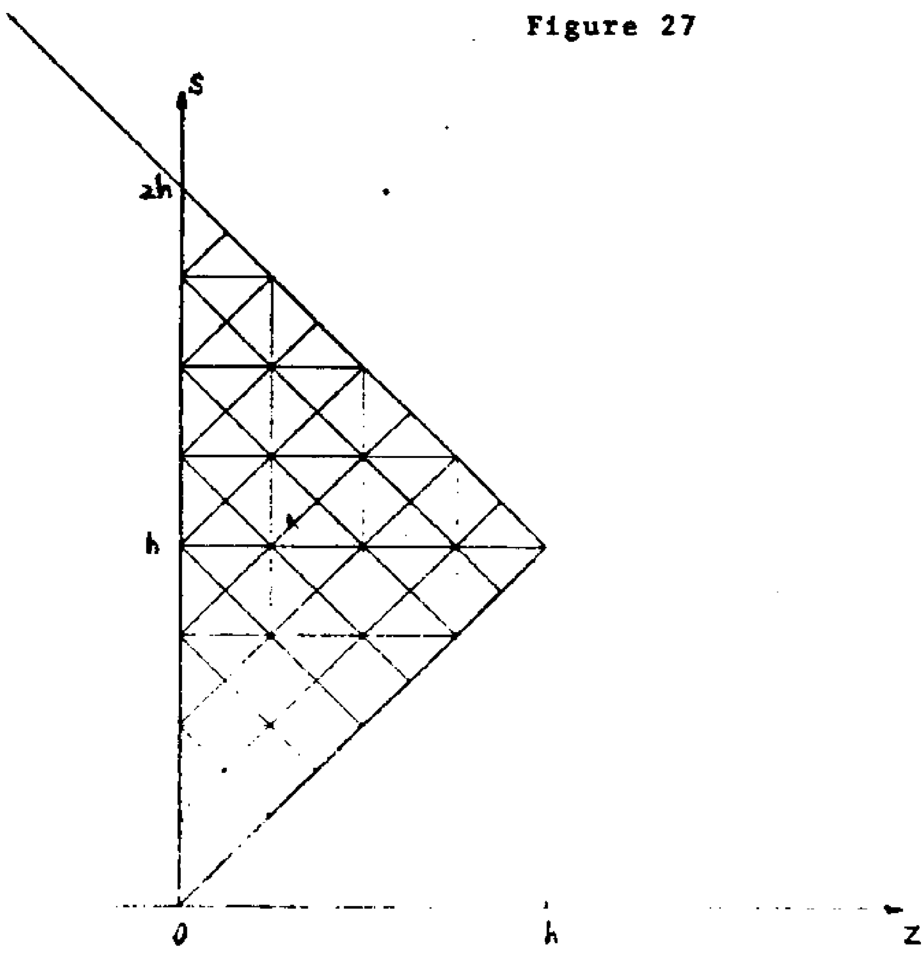

Figure 28